IEEE Access
Multidisciplinary ⋮ Rapid Review ⋮ Open Access Journal

Received February 14, 2022, accepted March 21, 2022, date of publication April 7, 2022, date of current version April 19, 2022.

Digital Object Identifier 10.1109/ACCESS.2022.3165594

GNSS User Technology: State-of-the-Art and Future Trends

DANIEL EGEA-ROCA[1], (Member, IEEE), MARKEL ARIZABALETA-DIEZ[2], THOMAS PANY[2], (Member, IEEE), FELIX ANTREICH[3], (Senior Member, IEEE), JOSÉ A. LÓPEZ-SALCEDO[1], (Senior Member, IEEE), MATTEO PAONNI[4], AND GONZALO SECO-GRANADOS[1], (Senior Member, IEEE)

[1]Department of Telecommunications and Systems Engineering, IEEC-CERES, Universitat Autònoma de Barcelona (UAB), 08193 Barcelona, Spain
[2]Institute of Space Technology and Space Applications (ISTA), Universität der Bundeswehr München, 85577 Neubiberg, Germany
[3]Aeronautics Institute of Technology (ITA), São José dos Campos 12228-900, Brazil
[4]European Commission, Joint Research Centre (JRC), I-21027 Ispra, Italy

Corresponding authors: Daniel Egea-Roca (daniel.egea@uab.es) and Markel Arizabaleta-Diez (markel.arizabaleta@unibw.de)

This work was supported in part by the Future Navigation and Timing Evolved Signals-2 (FUNTIMES-2) Project, through the European Commission, under Grant 630/PP/GRO/RCH/17/9877; in part by the Spanish Ministry of Science, Innovation and Universities, the Institució Catalana de Recerca i Estudis Avançats (ICREA) Academia Programme, under Project PID2020-118984GB-I00; in part by the Conselho Nacional de Desenvolvimento Científico e Tecnológico (CNPq)-Brazilian National Research Council under Grant 309248/2018-3 PQ-2; and in part by Universität der Bundeswehr München.

ABSTRACT Advances in the miniaturization, computational capabilities, and cost reduction of semiconductor technology have made global navigation satellite systems (GNSSs) the favorite choice for positioning. Currently, positioning is a key factor for many essential tasks in our modern society and will become even more important with the advent of new concepts such as the Internet of Things (IoT), smart cities and autonomous driving. The extensive use of GNSSs in a wide range of applications has caused their migration from the professional segment to the mass-market segment in terms of both technology and performance. This presents new and more stringent requirements in terms of accuracy, robustness, ubiquity, and continuity for the original ''open sky'' GNSS design. GNSS technology has experienced an unprecedented evolution in the last decade, and it is expected to exponentially evolve in the next decade. This evolution is considered in this paper with the aim of providing a unified reference for current GNSS receiver technologies and solutions and its expected evolution in the next decade. We consider receiver concepts, antennae, RF front ends, digital signal processing, and positioning algorithms. The impacts on the different GNSS market segments and applications are also analyzed.

INDEX TERMS Positioning, GNSS, user segment evolution, core technology, algorithms, receiver architecture.

I. INTRODUCTION

Over the last decade, the development of semiconductor technology has experienced exponential growth that has led to the miniaturization of components, the provision of higher computational capabilities, and the cost reduction of myriad electronic devices used in our daily life. In this new era of ubiquitous small electronic devices with high computational capabilities, the provision of localization and precise timing has become an important aspect of our modern society. Relevant examples include the most recent smartphones and modern vehicles, all of which are equipped with positioning modules able to provide user locations. Positioning and timing information are expected to have a greater impact in the future with the advent of 5G/6G communications [1], autonomous driving [2], the Internet of Things (IoT) [3] and smart cities [4].

Currently, global navigation satellite systems (GNSSs) are the favorite technology to provide positioning and timing capabilities in sectors such as surveying, remote sensing [5], object or animal tracking [6], and aviation [7]. Global navigation satellite systems provide unprecedented levels of accuracy for positioning with global coverage at any time and with reasonably low infrastructure costs. Thus, GNSSs are expected to play a primary role in the new era of applications to appear in the coming years. It is worth pointing out that traditional GNSS receivers are mostly used under open-sky conditions due to their technological limitations. However,

The associate editor coordinating the review of this manuscript and approving it for publication was Derek Abbott.

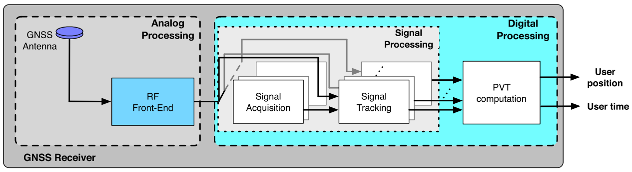

FIGURE 1. Block-level architecture of traditional GNSS receivers.

with the use of more complex algorithms and improved hardware technology, GNSSs can be used almost everywhere, with indoor positioning being one of the main challenges for today's GNSS technology [8].

In parallel with semiconductor technology, GNSSs have also experienced unprecedented growth in terms of both adoption and evolution of the technology since its origin. The first GNSS was the well-known Global Positioning System (GPS), developed during the early 1970s by the U.S. government and declared fully operational in 1995 [9]. The Russian system GLONASS was developed almost at the same time and was also fully operational by 1995 [10], [11]. Today, the European Galileo system and the Chinese BeiDou are also available for use [11]. India and Japan have also developed regional standalone (NavIC and QZSS, respectively) or augmentation systems [11]. The implementation of all these systems allow receivers to use satellites from different systems to compute the user position, namely multi-GNSS, and this is an additional key driving force for the popularization of GNSS. These systems provide the satellite constellation and ground segment equipment needed to control the proper behavior of the system that allow the user to obtain its position, velocity and time (PVT) solution.

For the PVT computation, traditional GNSS receivers have used first an analog processing to capture and digitize the GNSS signals. Second, the digital processing of the receiver identified the different satellites in view and extracted the information needed for the PVT computation. This has traditionally been done by the so-called acquisition and tracking module of the receiver. Then, the PVT computation module obtains the user solution given by 4 parameters: the user's 3D position coordinates and GNSS time [10]. This is why the acquisition and tracking modules are repeated for every satellite in view, usually at least four satellites. An overview of this architecture is given in Fig. 1.

Both the evolution of semiconductor technology and the aforementioned boost in GNSS system development have caused a rapid growth in the GNSS market from the professional to the mass-market (MM) segment. This has caused an unprecedented evolution of the traditional GNSS architecture and its uses. Nowadays, the PVT solution provided by a GNSS receiver can be used for many purposes. For instance, as positioning information like in animal tracking [6], [12], as timing information for communication network synchronization [13], [14], or as external information for a vehicle navigation system [2], just to mention a few. This advance in positioning technology additionally spurred very stringent user requirements in terms of accuracy, availability, and robustness, which could not have been fulfilled with the original GNSS technology. For this reason, GNSS user technology has evolved drastically from its origins to fulfill these different requirements in a very short time.

It is important to note that the specific user technology of each GNSS application is diverse and it is out of the scope of this paper. In this paper, we focus on the GNSS user technology defined by the components in Fig. 1 and its evolution. This includes evolution in both the core technology (i.e. hardware) as well as the signal processing, PVT module and the receiver and antenna architecture itself. The literature that highlights this evolution and illustrates its future path is broad and sparse. For instance, the hardware evolution includes different components, such as the antenna or the RF front end, which can be considered two separated fields. Therefore, the hardware evolution is covered in a wide variety of literature. Similarly, for the signal processing evolution, we find diffuse literature dealing with advances on the PVT algorithm, multipath mitigation and/or interference and spoofing detection. For receiver architecture, we find different alternatives such as cloud-based, snapshot and hybrid architectures.

In this paper, we provide a far-reaching overview of the state of the art and ongoing technological evolution in the field of GNSSs to fulfill the increasingly stringent requirements that will likely be imposed by a very wide spectrum of GNSS-based applications [15]. The goal is to unify this state of the art in a single contribution with a proper structure that allows us to discuss all important aspects of GNSSs. This will span from the hardware (HW) components used for the most basic tasks to the components used to run the software (SW) used for the most sophisticated tasks of a GNSS receiver. We perform a comprehensive review of the state-of-the-art signal processing algorithms expected to boost the accuracy, availability, and robustness of future GNSS receivers. We especially emphasize advanced precise positioning, multiantenna (MA) and hybridization algorithms, as they are considered key technology drivers of future evolution. Furthermore, future architectures, such as cloud-based and snapshot solutions, are considered to target low-power (LP) consumption or high sensitivity (HS). Before detailing each of these elements, let us first offer a brief introduction to GNSS technology and market evolution as well as the definition of the structure of this paper.

A. GNSS TECHNOLOGY EVOLUTION

From a user segment (i.e., the receiver) perspective, the proliferation of GNSS-based applications in many fields has produced diversification of the application-specific requirements to achieve a desired quality of service. One of the most common and continuously increasing demands is definitely on the accuracy side combined with long continuity. To achieve the most challenging levels of accuracy, carrier phase positioning must be targeted. Levels of accuracy reaching the sub-decimeter were demonstrated in the early 1980s, first revolutionizing geodesy and later surveying and machine control. Currently, carrier phase positioning is even more widespread thanks to the development of more cost-efficient user equipment and services. For instance, augmentation systems in the form of reference station networks provide the accurate corrections needed to generate the most accurate solutions [9], [11]. On the other hand, powerful measurement processing algorithms have been developed to estimate and resolve carrier phase ambiguities [10], [11].

To achieve the desired accuracy with long continuity, a key factor is represented by the use of multiconstellation (MC) and multifrequency (MF) receivers, already available in the MM segment since 2017 [16]. The use of MA solutions is also an option for improving GNSS measurements with respect to accuracy and continuity [17]. Indeed, the key factor that favors the inclusion of MC and MF capabilities or the use of MA solutions is semiconductor miniaturization, which leaves enough space in a receiver to add more components to the receiver chip (e.g., additional memory, processors or front ends making a receiver MF).

Following the same direction, GNSS receiver chipsets have evolved with respect to computationally complex algorithms, enabling higher sensitivity and accuracy. An example is in automotive technology, where several sensors and communication signals have been fused to aid GNSS signals to achieve more accurate position computations [18]. Unfortunately, current solutions delivering high accuracy (HA) and sensitivity are typically limited by their high energy consumption. This is not only due to the high complexity of the signal processing employed but also due to the limited size of the professional market. Two directions are expected to play a predominant role concerning the issues discussed above, i.e., cloud-based [19] and snapshot solutions [8].

Finally, there is a trend toward more robust and with higher integrity receivers. This trend is driven by applications that nowadays are becoming critical to our society. This critically comes in the form of safety-of-life for the user, legal aspects, or economic issues. Some examples of such applications are autonomous driving [2] or civil aviation [7], automatic road user charging [20] or pay-per-use insurance [21], [22], and power grid monitoring [14] or stock trading operations [14], respectively. Nowadays, timing receivers are used in many economically critical applications. For this reason, they are the ones leading the evolutionary path to more robust receivers and with more integrity.

B. GNSS MARKET EVOLUTION

Migration from a high-end professional segment to an MM segment, as introduced above, has been taking place since the 1990s [9], [23], [24]. Nevertheless, the impact and spread of the MM segment is expected to exponentially grow over the next decade [15], [25]. This is thanks to the widespread support for MC and the new trend of adoption of MF reception of GNSS signals [26], [27]. This provides a growth of new value-added services [15], especially HA services. Traditionally, these kinds of services have been mainly offered to professional users, but now they are reaching the realm of MM users. An additional trend is identified by the provision of both safe and secure critical PVT solutions. As highlighted in [25], this trend is especially important where PVT solutions will be at the core of systems in which humans are out of the control loop, such as in communication network synchronization, power grid monitoring, and autonomous vessels, cars or drones (urban air mobility). Upcoming Galileo authentication services, namely, the open service navigation message authentication (OSNMA) and the commercial authentication service (CAS), are expected to be important enablers for these solutions.

In addition to accuracy and robustness, there are other PVT technology drivers that are considered to provide the basis for a new generation of GNSS-based applications, such as ubiquity (operation in different environments), connectivity with other systems and integrity [15]. This perspective of the GNSS market segment is the benchmark of this paper, and it is based on each market segment identified in [15] and defined here as follows:

1) *Mass market (MM)*: characterized by high-volume receivers for consumer devices. This includes applications such as automotive uses (not safety-critical), consumer drones, smartphones, augmented reality, and specialized IoT devices from mHealth to robotics. The key performance parameters (KPIs) of MM receivers are low-power consumption increasingly targeting more accurate solutions. Accuracy of the order of meters are considered. Then, MM receivers provide such levels of accuracy but with the lowest power consumption possible (between 1.5 to 200 mW). It is important to note that MM receivers target a short time-to-first-fix (TTFF) ranging from a maximum of 30 s in a cold start to a maximum of 2 s for a hot start.
2) *Transport safety- and liability-critical (SCAp)*: characterized by receivers built in accordance with specific standards to deliver such solutions. Automotive, aviation, professional drones, urban air mobility, maritime, search and rescue, and space-borne GNSS applications are all covered. The use of the PVT solution in such applications is diverse, but all of them use a GNSS user technology targeting high levels of integrity and robustness. This is translated into medium levels of accuracy between 2.5 - 10 m and 4 - 20 m the 95% of the time for the horizontal and vertical planes, respectively. Integrity for safety-critical applications and robustness against multipath, unintentional interference, jamming and spoofing are all provided. In this case, the maximum TTFF is 120 s and 30 s for a cold and hot start, respectively.
3) *High precision and timing (Professional)*: Characterized by receivers designed to deliver the highest accuracy possible. Agriculture, geodesy, surveying, machine control, timing, and synchronization applications are all covered. The main target of the GNSS user technology in such applications is to obtain a PVT solution with the highest accuracy possible. In the last years, professional applications have also shown an

interest on integrity PVT solutions for safety-of-life and capital-intensive applications, e.g., machine control or mining. In the professional segment, it is desired to achieve a cm-level accuracy.

C. CONTRIBUTION AND STRUCTURE

This paper aims to provide a comprehensive overview of the technological evolution of GNSS user technology starting from the current state of the art. The goal is to bring together all important aspects into a single reference for developers of user applications and GNSS technology as well as users with a technical background. Moreover, this overview facilitates the understanding of the different directions GNSSs have evolved to and shows the unfolding future developments. We discuss the current and future challenges of GNSS technology as well as key solutions expected to play a predominant role in the coming years. Additionally, we provide a perspective of the current level of maturity as well as the adoption and benefits of each evolution trend in the future.

Based on these considerations and with the traditional GNSS user technology architecture in Fig. 1, the contribution of this paper is twofold. First, we provide a comprehensive overview of GNSS technology divided into three main blocks: (i) the core technology (i.e., HW) of each component in Fig. 1, (ii) the algorithmic part corresponding to the digital part of the receiver architecture in Fig. 1, and (iii) the receiver architecture, having as benchmark the one in Fig. 1. The task here is to disseminate the current state of the art of these three blocks as well as their expected evolution. Second, and more importantly, we aim to fill the gap between these three blocks, which have usually been treated separately in the literature. We do so by putting all the contributions together to provide a clear perspective of the evolutionary paths in GNSSs and how this will impact the market.

To do so, the rest of the paper is organized as follows: In Section II, we summarize the state of the art for these GNSS receivers and the evolution of these core technologies, including the basic algorithms needed to acquire the satellite's signals and to compute the PVT. This will be the basic setup used to describe the advanced algorithms and configurations considered in following sections. In particular, Section III addresses advanced signal processing algorithms that will boost the performance of future GNSS receivers. Then, Section IV assesses future receiver architecture evolution targeting LP and HS. Finally, Section V concludes the paper by providing a perspective on GNSS technology over the next decade based upon the discussion provided in this paper. That section also concludes with a list of current GNSS chipsets in the market as well as a summary of the concluding remarks we can extract from this paper. Due to the length of the paper and for the reader convenience, we provide in Table 1 a list of the used acronyms.

II. CORE TECHNOLOGY EVOLUTION

Let us start with the evolution of GNSS receiver core technology, including the basic HW and SW components

TABLE 1. List of acronyms.

A-GNSS	Assisted GNSS
ADC	Analog-to-Digital Converter
ARAIM	Advanced RAIM
ASIC	Application Specific Integrated Circuit
AWS	Amazon Web Services
BCH	Bose-Chaudhuri-Hocquenghem
CAS	Commercial Authentication Service
Chimera	Chip Message Robust Authentication
CRPA	Controlled Reception Pattern Antennas
CSAC	Chip Scale Atomic Clock
DLL	Delay-Lock Loop
DoA	Direction of Arrival
FDE	Fault Detection and Exclusion
FFT	Fast Fourier Transform
FLL	Frequency-Lock Loop
GNSS	Global Navigation Satellite System
GPS	Global Positioning System
HA	High Accuracy
HAS	High Accuracy Service
HS	High Sensitivity
HW	Hardware
IMU	Inertial Measurement Unit
INS	Inertial Navigation System
IoT	Internet of Things
IPPP	Integer PPP
ITAR	International Traffic in Arms Regulations
JSON	JavaScript Object Nation
KPI	Key Performance Indicator
LDPC	Low-Density Parity-Check
LEO	Low-Earth Orbit
LHCP	Left-Handed Circular Polarized
LNA	Low Noise Amplifier
LOS	Line of Sight
LP	Low-Power
LS	Least-Square
MA	Multiantenna
MC	Multiconstellation
MF	Multifrequency
MM	Mass-Market
NLOS	Non-Line of Sight
NMA	Navigation Message Authentication
NRTK	Network RTK
OCXO	Oven-Controlled crystal Oscillator
OSNMA	Open Service Navigation Message Authentication
PLL	Phase-Lock Loop
PPP	Precise Point Positioning
PVT	Position, Velocity and Time
RAIM	Receiver Autonomous Integrity Monitoring
RF-FE	Radio Frequency Front End
RHCP	Right-Handed Circular Polarized
RSS	Received Signal Strength
RTK	Real-Time Kinematics
SBRTK	Single-Baseline RTK
SCA	Spreading Code Authentication
SCAp	Safety- and liability-Critical Applications
SNR	Signal-to-Noise Ratio
SoO	Signal of Opportunity
SS	Solution Separation
STAP	Space-Time Adaptive Processing
SW	Software
SWaP	Size, Weight and Power
T-RAIM	Time-RAIM
TCXO	Temperature Compensated crystal Oscillator
TOA	Time of Arrival
TTFF	Time-to-First-Fix
UWB	UltraWide-Band
VT	Vector Tracking
WARTK	Wide-Area RTK

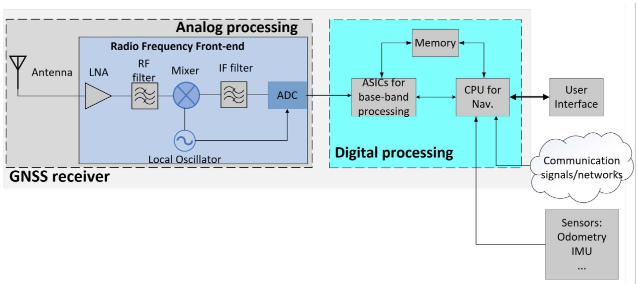

FIGURE 2. Core technology of a traditional GNSS receiver.

TABLE 2. GNSS antenna types and their characteristics [28].

Antenna type	Inherent BW	Multipath/Interference mitigation	Phase center stability	Size	Cost
Patch	Narrow	Medium / Medium	Medium-Poor	Small-Medium	Low
Quadrifilar helix	Narrow	Medium / Medium	Poor	Small-Medium	Medium
Cross slot/dipole	Narrow	Medium / Medium	Medium	Medium	Medium
Planar spiral	Very wide	Medium-High / Medium	Very good	Medium	Medium
Travelling -wave (TW) antenna	Very wide	Medium-High / Medium	Good-Very good	Medium-Small	Medium
4-element ring array	Narrow-Wide	Medium-High / Medium-High	Poor-Good	Large	Medium-High
Adaptive 2-element array	Narrow	Medium / Medium	Poor	Small-Medium	Low-Medium
Adaptive multi-element circular array	Narrow-Wide	High / Very High	Medium	Medium-Large	Very High

traditionally used in GNSS receivers. In this section, we describe traditional GNSS receiver solutions. More sophisticated algorithms and architectures will be considered in Section III and Section IV, respectively. We follow the structure of Fig. 1 and we consider the core technology given by the component-level architecture shown in Fig. 2.

The figure shows the analog part composed of the GNSS antenna and all the components forming the radio frequency front end (RF-FE). These are the HW components considered in this section and they are described in Section II-A and Section II-B, respectively. Then, the core technology of the digital part is composed in Fig. 2 by the SW elements considered in this section. This includes ASICs, CPU and memory components used for the signal processing and PVT computation tasks of the GNSS receiver. Furthermore, for the PVT computation, some algorithms use external information from sensors or communication signals to improve the performance of the PVT solution. All these aspects of the digital part of Fig. 2 are covered in detail in Section II-C. This will include the description of each component as well as the algorithms implemented by them.

Finally, Fig. 2 also shows how the PVT solution is fed to the user interface. This interface can provide feedback information to the PVT module and it depend on the application. This interface is out of the scope of the paper. In the following, we provide details on the rest of elements in Fig. 2 and their evolution, which is strongly linked to semiconductor miniaturization.

A. ANTENNA

The first evolution trends to be covered in this paper are related to the GNSS antenna, which is the first element of a GNSS receiver and thus the first element potentially impacting the performance of the receiver. Next, we provide an overview of the main GNSS antenna types and their characteristics, the antenna configurations, and the identified design challenges and trends. A summary is provided in Table 2, with an overview of the different antenna types available for GNSS receivers and their main characteristics such as type of inherent bandwidth, size, and cost.

1) ANTENNA TYPE, SIZE AND CUTOFF ANGLE

The most common antennas in GNSS receivers are patch antennas characterized by a wide range of variants, e.g., slot-loaded patch, stacked patch, and E-patch antennas [28]. The main advantages of patch antennas (or microstrip patch antennas) are low cost, low profile, small form factor, surface conformability, and moderate gain performance [11]. The main disadvantage is that they are resonant and thus inherently use narrow-band fields. Considering the receiver trends towards the reception of MF GNSS signals, considerable effort is required to increase the frequency range and the antenna bandwidth of patch antennas for GNSSs. A possible solution to cover several bands by using patch antennas is to stack more than one patch element on top of each other [11]. An alternate solution is to tolerate a reduced antenna gain in one frequency band (e.g., L5) by partly compensating the gain with aiding; a higher power channel (e.g., on L1) aids the signal tracking of the lower power channel (e.g., L5) [29]. An additional issue to be considered in the receiver design phase is that the patch antennas suffer from surface wave emissions, which is also considered the main disadvantage of this antenna type.

In Table 2, the antenna size is measured in terms of its dimensions in mm; a small antenna is understood to have all dimensions below 25 mm, while a large antenna is expected to have dimensions above 120 mm. When applicable, the antenna ground plane is considered part of the antenna when determining the antenna size. Regarding the antenna size, in contrast with most HW components, this is not directly affected by semiconductor miniaturization, as the antenna size, in general, is directly proportional to the wavelength of the desired signal. In fact, the miniaturization of the antenna causes resonance at lower frequencies, reducing the radiation efficiency and the antenna bandwidth [30]. Some of the methods available to reduce the antenna size (with a possible increase in weight and cost) include (1) loading the antenna with high permittivity and permeability materials such as substrates (e.g., ceramics); (2) adding capacitive and inductive loads; (3) meandering and folding the printed circuit antennas; and (4) implementing shorting pins and slots.

The antenna can also be considered a primary spatial filter. Actually, the antenna helps to elevate the signal-to-noise ratio (SNR) of the line of sight (LOS) and allows the receiver to suppress undesired effects such as multipath, interference and spoofing attacks. To mitigate these impairments, the antenna cutoff angle can be moved towards the zenith [28], which coincides with the availability of more satellites near the zenith. This trend is not considered for antennas built in devices with an unknown orientation (e.g., smartphones).

2) ANTENNA CONFIGURATION

Beyond the configuration of the cutoff angle, additional techniques used to reduce the effects of multipath and interference attacks are based on locating the following elements of high-performance antennas below their rim (i.e., the outer edge or margin) [28]: choke rings, resistive loadings, conducting ground planes, and metamaterials. Unfortunately, these changes affect the antenna design methodology and use case, and antennas can become bulky, heavy, and expensive. Therefore, these solutions are typically applied in the professional sector and to some extent in the SCAp sector. Antennas with built-in devices of an unknown orientation (e.g., smartphones) show a more omnidirectional gain pattern with little suppression of signals reflected from the ground. Antennas built into cars often have strict restrictions on size and shape and may exhibit an azimuth-asymmetric radiation pattern.

With respect to polarization, GNSS signals are transmitted as right-handed circular polarized (RHCP) signals, and receiver antennas are thus also RHCP to reduce the influence of the reflected signals. Mass-market antennas are an exception, as they may be realized as linear polarized antennas due to size constraints. Alternatives based on dual-polarization antennas with two outputs – RHCP and left-handed circular polarized (LHCP) – have recently received attention, as the ratio between RHCP and LHCP signal power is a good anti-spoofing indicator [31], [32]. Furthermore, the LHCP output can be useful to estimate channel conditions [33]. Nevertheless, dual-polarization antennas are not expected for MM receivers but may be used in SCAp or professional receivers. This kind of configuration can be considered an adaptive antenna, which is the state-of-the-art approach for interference, multipath, and spoofing suppression in GNSSs, and this will be described in Section III-B.

3) ANTENNA EVOLUTION PERSPECTIVE

The major challenges when designing antennas include bandwidth requirements, operating platform constraints, feeding networks, and cost. Furthermore, a symmetric and well-calibrated phase diagram is a key quality criterion. Among these challenges, the cost of the antenna is the main consideration driven by the market, and due to their characteristics, the previously mentioned patch antennas are the most widespread antennas used in GNSSs. Therefore, MM receivers are usually equipped with single passive antennas, supporting only the L1/E1 band.

In recent years, two different evolution trends have been identified: a single frequency GNSS antenna for low-power applications, and a multi-frequency antenna for MM applications without strict power constraints. The trend towards dual-frequency receivers has been observed with the release of receivers from Broadcom in 2017 [16], Qualcomm in 2019 [34], and Sony in 2020 [35]. These receiver releases show the trend of covering more GNSS bands. The second evolution trend can be observed in MM receivers as a result of the increasing number of IoT applications requiring GNSSs. The number of bands processed by a receiver becomes less important as the energy consumption is more relevant, i.e., single-frequency GNSS antennas are still expected to be employed in low-power GNSS receivers. As observed in [35], IoT chips can still work in several frequency bands; however, in applications requiring extremely low power consumption, single-frequency signal processing is expected to be employed, as shown in [36].

Notwithstanding, due to the increased burden on dual-frequency antennas and RF-FEs, in 2020, a single-frequency but L5-only receiver was additionally released for MM applications [36], thus leaving MF antennas to a more professional sector. A similar trend is emerging for MA configurations. To summarize the antenna evolution trend, in future years, triple-frequency antennas could be expected, not only in the professional and SCAp sectors but also in MM receivers without strict power constraints, as the line between MM applications and applications requiring HA is becoming blurred [15]. Size and form factors will be adapted to specific platforms (e.g., smartphones, chassis) and will eventually account for the orientation and local environment (e.g., human body interaction) of the platform to achieve a desired gain and phase diagram.

B. RF FRONT END (RF-FE)

We continue in this section with the structure with the component-level architecture shown in Fig. 2. After the antenna, the signal is processed by an RF-FE, which is composed of a low noise amplifier (LNA), an RF filter, a local oscillator, a mixer, and an analog-to-digital converter (ADC); as shown in Fig. 2. The two first elements (i.e., LNA and RF filter) are in charge of adapting the GNSS signal to be processed by the rest of the components. While the bandpass filter is employed to remove unwanted signals (out of band), the LNA is used to amplify the weak satellite signals plus noise from the antenna. In some instances, after the LNA a second filter is applied to provide additional filtering before the IF down-conversion and the digitization are performed. The RF-FE elements, discussed in more detail in this section, are the local oscillator and the ADC.

1) OSCILLATOR

Oscillators are a key element in GNSS receivers, as they provide the reference frequency and timing needed to process the GNSS signal [11]. They are first used in the RF-FE to down-convert the incoming RF signal into an IF or baseband signal. Furthermore, the oscillator provides the reference timing to the ADC to perform the sampling of the incoming

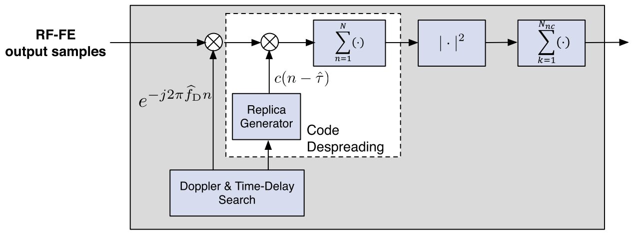

FIGURE 3. Correlation process to be implemented in ASICs for the signal processing part of the digital signal processing in a GNSS receiver.

signal during the digitization phase. Finally, the digital signal processing block shown in Fig. 2 provides both the reference time and frequency to generate the replica signals to be used in the signal processing (see Section II-C). Oscillator instabilities can cause errors in these reference signals, thus limiting receiver performance in terms of both user position and time.

The main operation to be carried out in the signal processing module is the correlation (see Fig. 3) of the input signal with a locally generated reference signal. As this is performed on a sample basis after the signal is digitized, the better the stability of the oscillator is, the longer the integration time that can be used for the correlation. Long integration times are specially required in HS or indoor scenarios, and therefore, oscillator noise is an important factor to be considered in an RF-FE since it limits the sensitivity and accuracy of the PVT solution [37].

Currently, the local oscillators employed in MM receivers are usually temperature compensated crystal oscillators (TCXOs) with a frequency offset ranging from 0.5 to 5 ppm [38], [39]. This frequency offset represents the instability of the oscillators. Common values of this frequency offset are provided in [40] for different types of low- and high-quality oscillators. The oven-controlled crystal oscillator (OCXO) provides a higher clock stability than the TCXO, the OCXO frequency offset ranges from 10^{-4} to 10^{-3} ppm [25]. However, to achieve this stability, OCXOs require a higher power supply, which is not compatible with small receivers such as MM receivers.

Oven-controlled crystal oscillators can be found in commercial-grade application boards. For critical infrastructure applications, however, rubidium-based oscillators are required [25], which are one of the most stable types of oscillators in the current market, reaching frequency offsets down to 10^{-11}. In recent years, chip-scale atomic clock (CSAC) technology has been developed, reaching also frequency offset to the level of 10^{-11}, with a much-reduced size [25]. The literature has already investigated the use of CSACs in GNSS receivers, showing a possible reduction in the minimum number of satellite signals received to three to compute the user position (this requires a calibration of the CSAC output frequency, and it is mandatory to synchronize the CSAC with the GNSS time) [41], [42] or to help mitigate multipath effects [42], [43]. Chip-scale atomic clock clocks provide a solution to the noisy short-term stability of current MM receiver clocks. It is worth noting that except for CSAC clocks, the stability of the oscillators used in current GNSS receivers is not enough to obtain HA positioning. For this reason, the user time is kept as unknown and subsequently computed in the PVT algorithm (see Section III-A).

2) ADC

The ADC is in charge of digitizing the data by performing sampling and quantization of the down-converted GNSS signal. As shown in Fig. 2, prior to reaching the ADC, the down-converted signal is filtered to remove unwanted components appearing during the down-conversion (i.e., intermodulation products). Then, the output of the ADC is a continuous stream of IF samples to be processed by an ASIC in the signal processing block of Fig. 2. The sampling and quantization processed from the ADC are directly linked to the memory and required processing power. The output of the ADC might be either a real or complex (I/Q) signal with sample rates between 5 and 60 Msps as a function of the frequency band of the desired signal that is being stored [44].

In addition to the sampling rates, the quantization level used in the ADC must also be considered, which might range from 1 to 16 bits per sample value. Standard ADCs provide many bits per sample, but many GNSS receivers use only 2 to 4 bits. This is sufficient to sample the dominant noise component within the GNSS signal. It is important to note that GNSS signals are spread-spectrum signals, so GNSS signal components have a much smaller amplitude than noise [11]. In cases of strong continuous interference being present, a highly linear front end (mixers and LNAs) plus many bits per sample are useful to detect such interference. In such a case, the ADC might apply up to 16 bits for each sample value [45]. Otherwise, the interference signal may saturate the ADC. In general, the use of higher quantization resolution implies that signal processing is performed with a higher number of bits; therefore, more memory and processing power is required. Additionally, the ADC itself consumes significantly more power for higher resolutions. Hence, current GNSS receivers are often designed to work at 1- or 2-bit quantization to reduce the required memory and power consumption.

3) RF-FE EVOLUTION PERSPECTIVE

Similar to the evolution trend of GNSS antennas, the RF-FE in MM receivers is associated with the low cost and low power requirements of the overall GNSS receiver. The main elements impacted by these requirements are the ones described above, i.e., the oscillators and the ADC. No large changes are expected in RF-FEs, including the addition of more RF-FEs within a receiver to cope with the expected increase in available frequency bands by the signal processing unit, e.g., ASICs. The oscillator quality in MM receivers is still expected to remain in the TCXO range (for MM receivers of the highest quality). The alternatives are very costly to employ in MM receivers or require high power consumption, which is not compatible with receivers requiring low power consumption, such as IoT devices. OCXO is expected to continue being employed in commercial boards, while atomic clocks and CSACs are expected to be oriented toward critical infrastructure.

Regarding ADCs, however, two main trends can be expected, especially for MM receivers. Those receivers requiring higher accuracies might benefit from using slightly higher sampling rates and quantization levels. However, the quantization levels will remain at 1 or 2 bits, and the sampling rate will be at a minimum for IoT receivers, in which the power consumption is the most relevant evolution criterion. Similarly, such receivers are expected to work in single-frequency mode, reducing the power consumption as much as possible. In other sectors, such as commercial receivers and/or in the professional and SCAp sector, the sampling rate is expected to be higher, as are the quantization levels. For these sectors, neither cost nor power consumption are critical points to be considered.

An alternative method usually employed in RF-FE signal processing is bandpass sampling. This method consists of down-converting the RF signal into a digital IF signal by directly sampling the RF signal bandwidth using intentional but nondestructive aliasing (i.e., the signal is directly sampled into a sampling frequency lower than that defined by the Nyquist theorem) [46]. The structure of the RF-FE consists of an RF filter to remove the noise of the signal coming through the RF antenna, an amplifier, an optional mixing stage, and a high-speed ADC that directly digitizes the incoming signal. The clock frequency and the band-selection filters allow for selecting the desired frequency band to down-convert from the received RF spectrum. The benefits of using bandpass sampling are that the analog part works at higher frequencies (e.g., at RFs or at high IFs of 50-200 MHz if one mixing stage is included). It should be noted that the sampling frequency is proportional to the information bandwidth rather than the carrier/intermediate frequency [47]. The main disadvantage is that the required sample and hold duration of the ADC is shorter than in other RF-FE structures. The bandwidth of the ADC must adapt the RF or IF, even when the sampling rate is much lower. The bandpass filter must also be designed with a steep roll-off, as it must attenuate all the energy (noise) outside the information bandwidth [47].

C. DIGITAL PROCESSING

Once the GNSS signal has been digitized, the digital part of the GNSS receiver is in charge of performing the main signal processing tasks and computing the PVT solution (see Fig. 1). The main signal processing tasks are signal acquisition and tracking, which are mostly implemented in application-specific integrated circuits (ASICs), as already indicated in Fig. 2. For the PVT computation, however, general purpose CPUs are used, and they become the critical element in each GNSS receiver being the boundary between hard real-time (ASIC) and soft real-time (CPU). The considerations of ASICs and CPUs used in GNSS are discussed in this section, as well as an overview of their evolution in a GNSS receiver.

1) ASICs: SIGNAL PROCESSING

Current GNSS receivers are mainly built-up in ASICs because they provide LP consumption with small size and low cost. The main operation required for digital signal processing is the correlation function shown in Fig. 3, which is used in both the acquisition and tracking modules of Fig. 1 and it is described next. From a signal processing point of view, GNSS receivers perform a very accurate synchronization. The synchronization required in a GNSS receiver is much higher than the synchronization required in communication systems, as 1 μs of error is translated into a ranging error of almost 300 m. This tight synchronization is performed in two steps. First, the signal is acquired, providing a rough synchronization. Then, the tracking module refines the synchronization. These two modules are further described in the following.

a: ACQUISITION MODULE

The first operation to be performed in a GNSS receiver when the signal has been digitized is signal acquisition, which means detecting the satellites in view. These satellites are used as the anchor points to compute the user's position in the PVT module. Furthermore, the key measurement needed for the PVT computation is also obtained in the acquisition stage, which is the measurement of the transmission time of the GNSS signal from the satellite to the receiver. To perform an accurate or at least a rough initial guess of the time delay, the Doppler frequency shift of the signal must also be estimated. Thus, the acquisition stage is forced to perform a two-dimensional (i.e., time-frequency) search [11].

The acquisition process in a GNSS receiver is usually performed in ASICs carrying out the correlation of the digitized GNSS signal with a locally generated replica. This process is shown in Fig. 3, and it consists of multiplying the input signal with the local replica for several time-delay and Doppler shift values. Then, this result is coherently added together for N signal samples. This process allows the receiver to despread the inherent code of the GNSS signal from the spread spectrum modulation [10]. This process is repeated for different code-delay and Doppler shift values, and if the correlation value is large enough, the signal is declared acquired with the corresponding time-delay and Doppler shift estimates. As discussed in Section II-B1, the maximum coherent integration time (i.e., T_{coh}) is limited by the oscillator quality. For this reason, as described in Fig. 3, the correlation integration time can be extended noncoherently by adding N_{nc} coherent integrations in case a more sensible or accurate solution is needed.

b: TRACKING MODULE

The tracking module of a GNSS receiver is in charge of refining and updating the coarse code-delay and Doppler shift estimates provided by the acquisition module. This is usually done by implementing two parallel closed-loop architectures in the ASIC, the so-called delay-lock loop (DLL) and phase-lock loop (PLL) [11]. These architectures are the same as those used in spread spectrum technology, and they are constructed with the same correlation structure given in Fig. 3. For applications in which less precision but more robustness is required, the PLL is replaced with a frequency-lock loop (FLL). In general, three different correlations are needed in a DLL and only one for the PLL/FLL. This indicates one of the most important differences with respect to the acquisition module in terms of energy consumption. Recall that a vast number of correlations are needed for acquisition, but only three are needed for tracking.

In today's GNSS receivers, it is considered that half of the overall chip power consumption is dedicated by ASIC processing, particularly when in acquisition mode [48]. As the number of applications requiring LP consumption has proliferated, manufacturers have focused on lowering power consumption at the expense of positioning performance. Some of the tracking methods employed to reduce power consumption include duty cycling [49], sub-Nyquist sampling [50] and channel multiplexing [51] combined with standard processing techniques (i.e., DLL and PLL). In terms of accuracy, one can observe a convergence of all receiver types towards the expected accuracy limit of tracking techniques. Even the super-low-cost ASICs in mobile phones provide geodetic quality output data that can be used for HA methods such as real-time kinematics (RTK) and precise point positioning (PPP). Today, it is apparent that the antenna is the element that creates the difference between an MM and a professional receiver.

Vector tracking (VT) is an advanced tracking method proposed to improve the performance of GNSS receivers [52]. Different from standard tracking, VT uses a Kalman filter as the PVT algorithm to estimate the navigation solution. Baseband processing results (i.e., PLL and DLL outputs) are employed to generate the input of the VT Kalman filter [52], [53]. The PVT solution is updated through the Kalman filter, and then it is fed back to the tracking loop to calculate the signal tracking parameters of the local replica. Different improvements in terms of an extended Kalman filter [54] or via the use of multiple receivers [55] have been proposed in the literature to improve the PVT solution provided by the Kalman filter used in VT. The main application of VT is in fading (challenging) environments, where the loss of lock easily occurs. However, the use of VT allows a fast reacquisition of the lost GNSS signals. Further applications are in ultratight integration with inertial navigation systems (INS). Such applications require high power consumption; therefore, this is not a suitable technique for LP receivers. Additionally, the implementation complexity for real-time applications should be considered due to the large amounts of data required to be immediately processed.

2) CPUs: PVT COMPUTATION

Position, velocity and time computation requires a number of different mathematical algorithms and partly extensive

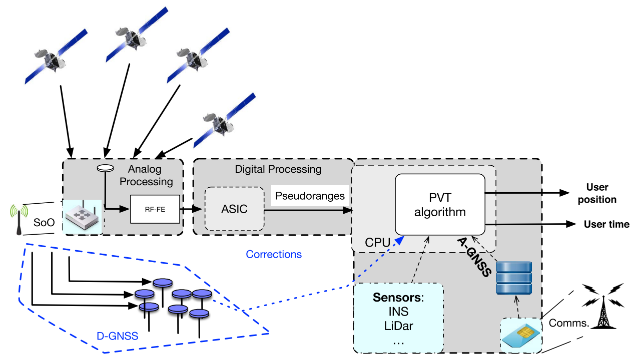

FIGURE 4. Traditional PVT module to be implemented in a general-purpose CPU for the PVT computation in a GNSS receiver.

linear algebra (i.e., matrix) operations. This is done best on a general-purpose CPU with floating point capability. A dedicated CPU can be used (e.g., for stand-alone GNSS receivers), or the CPU of the host system (e.g., smartphone) might be used. The GNSS SW on the CPU (=firmware) configures the ASIC controls for its real-time operation. This may range from receiving only GNSS observations (e.g., time delay, Doppler) in regular intervals up to direct control of the correlation process and receiver correlation values. To achieve this result, the CPU may have a data link to receiver assistance data or data from other sensors (see Section III-C). Different PVT computation options can be identified, such as stand-alone, RTK/PPP or sensor fusion.

a: PVT MODULE

A general PVT processing unit is given in Fig. 4. The first step is to capture and adapt the GNSS signal by the analog processing of the GNSS receiver. Then, the signal processing part carried out by the ASIC provides the pseudoranges to the PVT module. The PVT solution is resolved with linear algebra by the receiver's CPU. Errors in the pseudorange measurement and parameter modeling (e.g., ionosphere, troposphere, or multipath model) directly affect the PVT solution. To reduce these errors, differential position (or D-GNSS) methods are used [11]. An example of this case is shown in Fig. 4 as a nearby GNSS receiver at a known location that computes the errors affecting the GNSS signal. Then, the errors are provided to the user GNSS receiver for compensation.

Differential positioning or D-GNSS works for global effects such as atmospheric effects. Unfortunately, local effects such as multipath cannot be mitigated with the use of differential corrections. The Kalman filter can be used to reduce such errors. The use of the Kalman filters provides an alternative also to generic least-squares solutions to reduce or mitigate multipath induced errors at measurement (PVT) level, especially if the Kalman filter exploits Doppler observations, as they are much less impacted by multipath. The Kalman filter has also been used to improve the traditional standard positioning performance, beyond reducing the effects of multipath. Indeed, Kalman filters can improve positioning performance by incorporating past measurements and an adequate system model or by incorporating additional measurements from external systems (i.e., sensor or data fusion). As illustrated in Fig. 4, these external systems might range from sensors, such as odometry sensors, inertial measurement units (IMUs), or magnetometers, to communication networks such as 4G and 5G or other communication signals, mostly so-called signals of opportunity (SoOs). The algorithms used to combine these external systems are called hybrid algorithms and are covered in Section III-C. The use of such algorithms not only provides a higher accuracy to the computed position but can also be used to achieve higher integrity (understood as robustness).

b: PVT ALGORITHM

Let us describe the linear algebra implemented in the CPU of the GNSS receiver to use the PVT algorithm in Fig. 4 that computes the PVT solution. As GNSS positioning uses time of arrival (TOA)-based positioning [10], the GNSS receiver must compute the signal propagation delay between each satellite and the receiver. In other words, to obtain the user's position, GNSS receivers have to first estimate the time delay of the received signals from each visible satellite. Specifically, the receiver obtains a range measurement that for the i-th satellite can be modeled as

$$\rho_i = c\Delta\tau_i = r_i + c\delta t_\mathrm{u} + \epsilon, \qquad (1)$$

where c is the speed of light, $\Delta\tau_i$ is the i-th time-delay measurement, r_i is the true geometric distance between the i-th satellite and receiver, δt_u is the user's clock bias (with respect to the satellite's clock) and ϵ denotes additional errors (e.g., ionospheric and tropospheric propagation delays) to be considered in the position computation. In the GNSS literature, ρ_i is referred to as pseudorange because it is a measure of the distance but shifted by the unknown quantity $c\delta t_\mathrm{u}$.

These measures are the ones provided by the acquisition/tracking stage to the PVT module with the aim of estimating the user position and time (i.e., PVT), $\boldsymbol{r}_\mathrm{u} = [x_\mathrm{u}, y_\mathrm{u}, z_\mathrm{u}, c\delta t_\mathrm{u}]^\top$. Note that the clock bias is included as an additional unknown for the PVT computation. Then, we can rewrite (1) as

$$\rho_i = \sqrt{(x_j - x_\mathrm{u})^2 + (y_j - y_\mathrm{u})^2 + (z_i - x_\mathrm{u})^2} + c\delta t_\mathrm{u} + \epsilon, \qquad (2)$$

with $\boldsymbol{s}_i = [x_i, y_i, z_i]^\top$ being the coordinates of the i-th satellite. These coordinates are known to the receiver since they are provided within the navigation message of the GNSS signal. Thus, after the linearization of (2), the PVT solution can be obtained as a linear problem with 4 unknowns: the 3D coordinates and the user's clock bias. This means that signals from at least four satellites need to be received to resolve the unknowns. Different methods to obtain the PVT may be found, such as closed-form solutions, epoch-per-epoch least squares adjustment, or Kalman filtering [11].

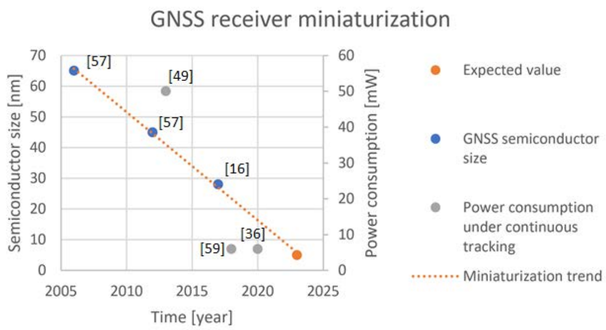

FIGURE 5. Evolution trend of semiconductor miniaturization in state-of-the-art MM GNSS receivers.

3) EVOLUTION PERSPECTIVE

The main evolution trend observed in signal processing is semiconductor miniaturization, following Moore's law. In 1993, GNSS receivers were built with few correlators, limiting the search of satellites to one time delay at a time (i.e., serial search). The acquisition at this point was slow and only successful for the cases in which the received signal was strong, i.e., outdoor scenarios with clear LOS signals [56]. Years later, with the introduction of E-911 [56], the receivers were forced to use larger amounts of correlators, allowing a parallel search. This was conceived thanks to the ASIC evolution that allowed the introduction of a bank of correlators within the GNSS receivers. With the advances of the semiconductor industry and its related progress on ASICs, the memory increased proportionally to the computational capacity to store and accumulate all the search-space hypotheses in parallel. Currently, GNSS receivers work by applying massive parallel correlations. To reduce the required memory, the fast Fourier transform (FFT) is applied to perform the correlation operation described in Fig. 3 [57]. Despite the fact that the use of FFT helps to reduce the size of the ASIC chip (i.e., a lower number of gates is required), memory has become the dominant factor of GNSS chip cost and size [56]. Memory is needed to accumulate correlation values during acquisition for all time-delay and Doppler values and for several noncoherent integrations (see Fig. 3).

From a market perspective, since 2017, new GNSS MM receivers have already supported dual-frequency and MC signals for positioning. As the line between MM applications and professional applications is becoming blurred with applications such as smartwatches, mHealth and drones, in the future, triple-frequency receivers are expected to be employed not only in professional and SCAp applications but also in MM applications. This is due to semiconductor miniaturization, which allows the computational and memory requirements of these applications in an MM to be fulfilled. Both Moore's and Koomey's law apply to ASIC technology. Fig. 5 shows the evolution trend of state-of-the-art MM chip semiconductor technology. The figure shows the trend of both semiconductor size and power consumption. By following this trend, the semiconductor technology in MM GNSS chips is expected to be reduced by another 20 nm by 2023, as achieved by the Qualcomm Snapdragon 855 Mobile Platform chip released in January 2019 [34]. The CPU of this chip was manufactured by processing technology as small as 7 nm.

A reduction in the semiconductor size implies a reduction in the chip size or can be observed as additional space in the chip to add further devices, e.g., an additional processor for applications in which additional processing power is required, memory for applications with high storage requirements (e.g., signal authentication), space for INSs, or MA systems. Furthermore, a trend to minimize the power consumption of the baseband processing can be observed from the computational power point of view. The reduction in power consumption is shown in Fig. 5 for continuous tracking. Lower power consumption is also observed in cases of duty-cycled tracking; e.g., in 2013, the state-of-the-art GNSS chipsets had a power consumption on the order of 15 mW for duty-cycled tracking [48]. In 2020, continuous tracking of 6 mW was achieved in two new HA dual-frequency GNSS receivers using only single-frequency processing in the L-band and between 9 and 11 mW by using the dual-frequency capability [35].

III. SIGNAL PROCESSING AND PVT ALGORITHM EVOLUTION

Beyond the components and their evolution, as studied in Section II, the signal processing algorithms used in the digital processor need to be considered. This ranges from basic signal processing and PVT computation to future authentication or MA processing. However, in recent years, due to the advent of new GNSS-based applications, a high degree of accuracy is required even in challenging environments in which not enough GNSS signals are available to compute the user position. To address these issues, hybrid algorithms are employed, i.e., the information from GNSS signals is combined with information from additional sensors and/or communication networks to achieve higher position availability and accuracy.

Similarly, we have to consider the algorithm evolution in terms of robustness so that high availability and accuracy can be obtained in any environment. To do so, signal processing algorithms have been developed to detect and mitigate the main threats to a GNSS receiver. In particular, large efforts have been placed on the evolution of algorithms for the mitigation of these threats. The threats to a GNSS receiver may be natural effects such as multipaths or man-made effects such as RF interference. The latter may be caused by jamming or spoofing. Different techniques exist for the different threats, and they can be classified as precorrelation, postcorrelation and PVT level techniques. The evolution of these algorithms are considered in this section. We highlight here the main concepts and techniques used for mitigation; extensive reviews can be found in the literature [59]–[64]. Similarly, for detection techniques, reviews are provided in [65]–[67].

This section summarizes the current status of SW and algorithms implemented within a GNSS receiver, and it is structured as follows: Section III-A provides an overview of the evolution of PVT algorithms. Next, Section III-B reviews array signal processing techniques that can be implemented in MA systems. Finally, Section III-C considers hybrid solutions based on the combination of GNSSs with different alternatives such as INS, 5G communications, and SoO.

A. PVT ALGORITHMS

Let us first discuss various GNSS algorithms impacting the PVT algorithm, such as authentication algorithms, integrity algorithms and HA positioning algorithms.

1) AUTHENTICATION ALGORITHMS

In the near future, GNSS satellites are expected to provide authentication capabilities to GNSS receivers. Currently, Galileo and GPS have already defined their signal authentication proposals, the OSNMA [68] and chip-message robust authentication (Chimera) [69], respectively. In fact, the literature provides many authentication methods; however, the main techniques defined are navigation message authentication (NMA) and spreading code authentication (SCA) techniques [70], [71]. Both techniques are based on private-public key algorithms to encrypt the GNSS navigation message for NMA or the spreading code for SCA.

For authentication, the public keys associated with the satellite private keys are expected to be initially stored in the receiver. If the private key of the satellites is compromised, a key management routine is required to provide the public keys associated with the new satellite private key. To perform the authentication functions, receivers require further memory and processing power. Assuming a GNSS receiver implements both NMA and SCA, the memory requirements are impacted by the receiver sampling frequency, the quantization level, and the spreading code recording time. For instance, a receiver working at 4 Msps, 1 bit quantization, and requiring a snapshot of 100 ms would require an extra memory of 50 kB per satellite spreading code to be authenticated. Additionally, if at least four satellites have to be authenticated to achieve an authenticated PVT, a minimum of an additional 200 kB is required for SCA only. The required additional processing also needs to be considered, as it limits the number of GNSS receiver types hosting authentication functions. For example, battery-driven IoT devices are not expected to compute the authentication functions by themselves; however, these can be carried out via cloud computing (see Section IV-B).

RF fingerprinting is a new concept related to GNSS authentication that has become popular in recent years. RF fingerprinting is the process of gathering information about an electronic device to generate specific signatures that can identify the device itself [72]. The most common metrics for fingerprinting the device are those computed from the receiver clock drift [73], but other metrics, such as those based on GNSS measurements or velocity, can be used [72].

After selecting a proper set of candidate features, it is necessary to apply a feature selection algorithm that allows the authentication of the device.

2) INTEGRITY ALGORITHMS

The use of GNSSs in the civil sector have increased integrity requirements in some applications, especially in safety-critical sectors (e.g., aviation). Integrity refers to the ability of the user receiver to guarantee the quality and trust of the information supplied by a navigation system. Global navigation satellite system integrity was originally devised for aviation purposes [74]; currently, this concept is also crucial in other sectors such as autonomous driving. In particular, since its origins back in the 1980s, various augmentation systems have been developed. Examples include the so-called receiver autonomous approaches as well as satellite-based or ground-based augmentation systems, SBASs and GBASs [74]. The concept of such systems is either to use consistency checks or to combine the GNSS signals with augmentation information coming from satellites or ground stations (in SBAS and GBAS, respectively). The augmentation information is based on the estimation of the common-mode errors and fault detection capabilities. SBAS systems are usually deployed to cover very large areas, e.g., a whole continent, whereas GBAS covers small areas, e.g., an airport.

Within the context of aviation, very specific faults (i.e., code pseudorange biases) of the satellite system (basically only GPS was used) were assumed, and for the user receiver and antenna, strict installation and operation rules were enforced. Under these assumptions, autonomous integrity monitoring algorithms based on the redundant information within the GNSS constellation were developed. Such algorithms are commonly known as receiver autonomous integrity monitoring (RAIM). Several RAIM schemes have been proposed, such as least-square (LS) residual RAIM, solution separation (SS) RAIM, and Kalman filter-based RAIM/fault detection and fault exclusion (FDE) schemes. Among the RAIM techniques, the most basic RAIM algorithms focus on performing only fault detection, while more extended RAIM techniques are capable of performing FDE; when a faulty satellite is detected, this can be removed, and a position solution with integrity can still be provided to the user.

Advanced RAIM (ARAIM) is a systematic extension of this approach and considers dual-frequency measurements, more than one GNSS (i.e. GPS plus Galileo), many different failure modes and time-varying GNSS performance parameters (so-called integrity support message (ISM)) [11]. However, it must be noted that SBAS/GBAS information is useful to reduce the errors and detect faults due to global effects (i.e., errors coming from the GNSS itself), but it is not directly applicable for local effects such as interference and/or multipaths. Autonomous integrity monitoring (RAIM/ARAIM) provide local effects detection capabilities up to some extent, but in very controlled environments such as the aeronautical one [11]. For this reason, both SBAS/GBAS and RAIM/ARAIM are certified and extensively used only for applications in open-sky conditions, such as civil aviation. Unfortunately, in more challenging conditions, such as in urban environments, traditional augmentation systems fail to provide enough level of integrity due to multipaths, non-line-of-sight (NLOS) scenarios and limited satellite visibility. There is much ongoing research to extend these methodologies from aviation to other safety-critical applications under degraded signal conditions (e.g., autonomous driving). At this point, even if augmentation systems or RAIMs are employed in receivers for integrity purposes, multipath detection and mitigation still might be required.

Some of the most advanced RAIM algorithms might be capable of detecting and mitigating multipaths at the PVT level up to a certain level. Among further possible techniques, the simplest technique is elevation angle-dependent measurement weighting, which can be simply performed by using a least-squares solution or more sophisticated Kalman filter solutions [11]. More complex multipath mitigation techniques often monitor the presence of multipaths in the measurements (e.g., fluctuations in the signal power indicate fading and multipaths). This monitoring at the measurement level can be later used to exclude or deweight the measurement into the PVT algorithm. For measurement weighting, we note some of the many multipath mitigation techniques employed at the PVT level [11]. Regarding detection techniques, we note several useful measurements to detect multipaths and then exclude them from the PVT computation [65]–[67]. This kind of detection and exclusion technique is commonly referred to in the literature as *signal-level integrity* [75]. Similarly, hybrid solutions described in Section III-C are useful to mitigate multipaths at the PVT level. For instance, external sensors such as cameras, maps or IMUs have been extensively used to reduce multipath effects into PVT computations by excluding or weighting the measurements affected by multipaths [76]–[78]. Similarly, the combination of GNSSs and other communication signals combined with proper measurement weighting is shown to reduce the effects of multipath/NLOS into the PVT solution [79].

Finally, it is worth mentioning the RAIM version for timing receivers, that is, time-RAIM (T-RAIM) algorithms. These algorithms assess the reliability of the timing solution provided by a GNSS timing receiver [80]. Several solutions have been investigated, such as the basic T-RAIM based on pseudorange residuals [81] and the more sophisticated algorithm designed in [82] based on an MC solution. T-RAIM algorithms have also been considered for jamming and spoofing detection for timing receivers [83].

3) PRECISE POSITIONING

Standard positioning (defined in II-C2b) uses pseudoranges computed from the code phase of the spread spectrum modulation. The main difference of precise positioning is that it additionally uses carrier phase measurements. Carrier phase measurements were first explored in the 1980s and were

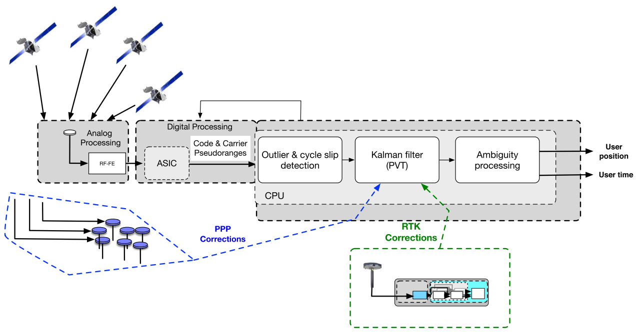

FIGURE 6. Block diagram of RTK/PPP-based positioning.

shown to provide levels of measurement accuracy up to the millimeter level that translated at that time to decimeter positioning accuracy. Today, carrier phase-based positioning is widely employed due to technological advances in the navigation field, particularly due to advances in D-GNSS and in the evolution of the implemented algorithms to resolve the PVT. Two of the best known techniques for HA positioning are PPP and the RTK, which are conceptually described in Fig. 6. The use of carrier phase measurements complicates receiver processing, as the following difficulties can arise:

- cycle slips in the carrier phase must be detected and corrected
- antenna phase center variations must be known precisely
- carrier phase observations must be continuously available over a reasonable time span

Let us focus first on PPP. Precise point positioning is a standalone positioning technique, and the main difference with respect to standard positioning is that it replaces broadcast satellite orbits and clocks with precise estimates. These precise estimates are produced by a widespread network of reference stations set by the PPP providers. The networks are used to accurately estimate the satellite orbits and clock errors and to directly provide the information to the user. These data are used by the user instead of demodulating the navigation data. To remove nearly all ionospheric propagation delays, dual-frequency data are usually combined. Furthermore, the receiver is required to compensate for other biases and non-integer ambiguity offsets of the IF combination of the carrier phase wavelength of the two signal frequencies.

On the other hand, the tropospheric propagation delay is a function of the tropospheric refractive index, which depends on the local temperature, pressure, and relative humidity; therefore, the propagation path length can be calculated in terms of refractivity. This term is often modeled by including a dry (or hydrostatic) and a wet (or nonhydrostatic) component [11]. The dry component can be rather accurately predicted. In contrast, the wet component arises from water vapor, and it is more difficult to predict due to uncertainties in the atmospheric distribution. Tropospheric delays are often computed as the zenith tropospheric delay of the dry and wet components multiplied by a so-called mapping function to express the elevation dependence. Then, the unknown PPP parameters include receiver coordinates, receiver clocks, zenith tropospheric parameters, and carrier phase ambiguities [11].

RTK is a differential positioning method that relies on resolving the carrier phase ambiguities to estimate the receiver position with HA. The use of carrier phase observations provides more precise navigation solutions. Real-time kinematics use a reference station and a rover receiver. However, this model is limited by the distance between the reference station and the rover. Some biases such as ionospheric signal refraction, orbit errors, and tropospheric refraction are distance-dependent. This delimits the use of RTK to a distance between the reference station and the rover of 10-20 km to resolve rapidly and reliably the carrier-phase ambiguities [11]. Real-time kinematics take advantage of a number of reference stations, which should not exceed 100-200 km, to produce highly accurate real-time correction models of the distance-dependent errors.

Fig. 6 shows the block diagram of the precise positioning algorithm. To perform PPP or RTK positioning, the PVT block uses as input the code pseudorange, the carrier phase of all tracked signals, and the PPP or RTK correction data. First, outlier detection is achieved, and if any is detected, this means that a false lock occurred, and this is transmitted to the tracking control. Afterwards, the receiver will check if any cycle slip occurred, and when detected, this is corrected or mitigated. Then, a Kalman filter is employed to reduce the biases induced by the atmospheric effects and resolve the PVT. Finally, the carrier phase ambiguities are estimated, validated, and fixed, achieving an HA PVT solution. Successful ambiguity resolution requires that all biases are known or estimated to a fraction of the wavelength (i.e., several millimeters max), and this includes all biases from the antenna or from MA processing. Furthermore, accurate pseudorange measurements (i.e., few or no multipaths) are required to ensure quick convergence of the float ambiguities to their integer values. Most of the PPP and RTK services identified in this section are provided by using terrestrial signals. Recent evolution of the GNSS systems suggest that PPP-related information is planned to be transmitted via satellite signals. Some examples are the already planned Galileo E6 high accuracy service (HAS) [84], and the BeiDou PPP-B2b service planned for the BDS-3 [85]. Additionally, commercial services exist providing PPP correction data via satellite [86], [87].

An overview of the accuracy that can be obtained with different high-precision techniques, depending on the baseline distance, is shown in Fig. 7. It is observed that the maximum accuracy is attained by single-baseline RTK (SBRTK) or employing network RTK (NRTK) positioning, but this can only be used with short baselines (below 40 km). The accuracy can reach 1 cm for baselines below 10 km, and it degrades up to 10 cm for baselines at approximately 40 km. Then, we must use PPP or integer PPP (IPPP) positioning, which gives an accuracy of approximately 10 cm in real-time processing and is even lower at postprocessing

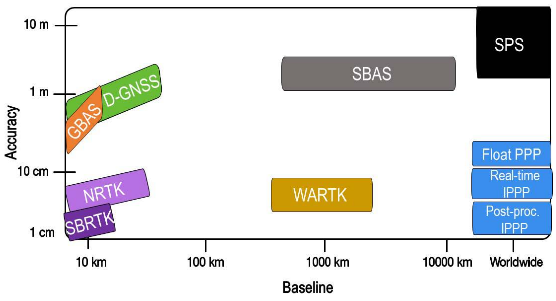

FIGURE 7. Accuracy overview for different GNSS positioning modes.

and is independent of the baseline distance. For comparison, traditional D-GNSS provides accuracy on the order of meters for baselines below 100 km. Standalone GNSS provides accuracy on the order of 10 m worldwide. Occasionally, baselines of several hundred kilometers are employed with techniques such as wide-area RTK (WARTK) and SBAS systems, which are expected to be used to achieve sub-10 cm and several meter accuracies, respectively. Among the presented techniques, it must be noted that all techniques are designed as real-time processing techniques but can also be applied in postprocessing, often reaching even higher accuracies. It must be noted that even several techniques exist to achieve precise positioning, standard positioning is still expected to be employed in future standalone receivers or receivers with low power requirements.

B. MULTI-ANTENNA ALGORITHMS

The use of multiple antennas as a group of sensors introduces sampling the received wave front in the time domain as well as the spatial domain. Hence, MA GNSS receivers enable the use of so-called array signal processing algorithms, especially for resilient GNSS positioning including multipath, interference, jamming, and spoofing suppression. Two main design strategies for GNSS MA receivers can be distinguished: tight and loose integration. In the case of *loose integration*, an additional system including the antenna array and the related signal processing is introduced before the input of a conventional single-antenna GNSS receiver (i.e., before correlation). On the other hand, in the case of *tight integration*, array processing algorithms can be applied before and after correlation, which provides more flexibility.

Next, we provide details on these configurations as well as different array processing algorithms that can be applied. Finally, evolution trends are provided.

1) RECEIVER DESIGN

In earlier days, loose integration was widely used for military applications. Spatial decorrelation or prewhitening filters were applied before correlation to suppress interference and jamming sources [88]. Although such approaches are very robust and efficient, in general, they cannot mitigate signals that are correlated with the desired satellite signals, such as multipaths or spoofing. These systems, which are called controlled reception pattern antennas (CRPAs), introduce one spatial filter that suppresses the interference or jamming signals and can enhance the SNR of the desired signals received from the satellites as much as possible. In general, this spatial filter is designed adaptively with respect to the changing signal environment. On the other hand, for tight integration, algorithms can be applied either before or after correlation. Algorithms that are applied before correlation affect all received signals, while algorithms that are applied after correlation can be tailored to each channel (i.e., satellite) individually.

In general, signals that are undesired and uncorrelated with the LOS satellite signals, i.e., interference and jamming, are suppressed before correlation, as for the loose integration. The undesired signals that are correlated with the LOS satellite signals, i.e., multipath and spoofing, are mitigated after correlation. More advanced structures of tight integration include the use of banks of correlators at each antenna output of the antenna array [89]–[91]. This provides even larger flexibility in signal processing and enables the use of space-time signal processing [89], [92], tensor-based signal processing [90], [93] or multidimensional signal processing [91], [94]–[96]. An overview of examples of currently available military systems can be found in [97]. Commercially available loose integrated CRPA systems use only a few antenna elements, e.g., two or three, due to international traffic in arms regulations (ITAR) restrictions, e.g., the GPSDome [98], but an increasing number of ITAR-free systems, even for SCAp, have been proposed and developed, e.g., [99]. In contrast, tight integration strategies have been studied extensively in recent years but are not yet commercially available.

One important practical aspect of any type of MA system is its calibration. First, the different RF-FEs for each antenna element need to be calibrated with respect to their relative phases and group delays. Second, precise knowledge of the 3D array response (single element embedded patterns) is vital for high-resolution spatial parameter estimation as well as to avoid so-called phase center variations [92], [100], [101]. Unfortunately, in many cases, the calibration will not be perfect, and thus, some errors will remain. Hence, robust array processing algorithms must be considered. Some of these algorithms rely solely on adaptive subspace decomposition to separate undesirable signals from LOS satellite signals [89], [92], [102], [103]. These types of algorithms are often called *blind* because they do not need any knowledge about the array response or the number of antennas.

2) MITIGATION ALGORITHMS

The quality of the ranging data provided by a GNSS receiver largely depends on the synchronization error, i.e., on the accuracy of the propagation time-delay estimation of the LOS signal received from the GNSS constellation. If the LOS signal is corrupted by multipaths, jamming, or spoofing as well as ionospheric propagation effects, the estimation of the propagation time delay or the carrier phase and thus positioning can be severely degraded or even denied. Therefore, new mitigation techniques for these effects have been proposed and studied for many years. Usually, jamming and RF interference are mitigated before the correlation process, whereas multipath and spoofing are mitigated after the correlation process. Precorrelation techniques are mainly based on MA algorithms or traditional single-antenna techniques for jamming mitigation [59], [60]. Postcorrelation techniques are also based on MA algorithms or traditional single-antenna techniques for multipath [61], [62] and spoofing mitigation [63], [64]. Position, velocity and time (PVT)-level algorithms were considered in Section III-A2.

Many single-antenna receiver techniques have been proposed to suppress interference or jamming, from notch filters to time-frequency filtering to subspace-based methods [59], [104]. However, in cases where the interference or the jamming is continuous, wideband, and of the same polarization as the GNSS signals, interference suppression with a single-antenna system is very limited [59]. Similarly, many techniques have been proposed for spoofing suppression and multipath mitigation. For spoofing, techniques have been developed for specific types of attacks [63], [64], [105]. However, when spoofing is received together with multipath or other propagation effects such as ionospheric scintillations, detection and separation of spoofing from these effects becomes difficult in a single-antenna receiver [63], [64].

For multipath mitigation, many techniques have been proposed using a single antenna, starting from classic correlator-based and multiple correlator-based methods [106] to Bayesian approaches [107], [108] and methods that estimate the distribution of multipaths and thus exploit multipaths to enhance positioning [109]. Incorporating several frequency bands, a bank of correlators for each satellite, and Bayesian estimation provides great capabilities to mitigate multipaths, but this pales in comparison with the possibilities introducing the spatial domain [110]. In the following, we discuss interference and jamming suppression as well as spoofing and multipath mitigation using array processing algorithms that provide advanced resilience. An overview of these techniques is shown in Fig. 8. Here, performance is related to each column, while complexity is indicated comparing the different approaches of all columns. Fig. 8 also shows which array processing algorithms can be used for loose and tight integration and whether they are applied before or after correlation.

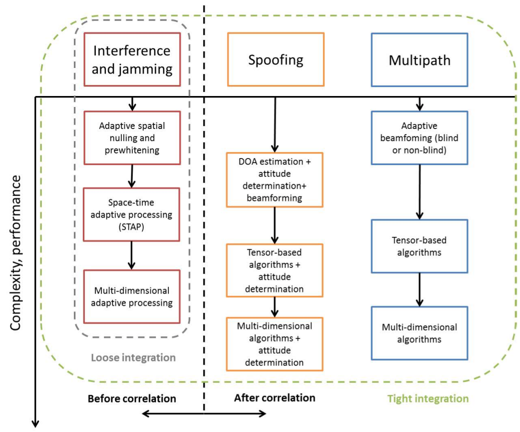

FIGURE 8. Overview of array processing algorithms with respect to complexity and performance.

a: INTERFERENCE AND JAMMING

Introducing spatial filtering [111], prewhitening (spatial decorrelation) [112], or joint space-time prewhitening [113] using an MA receiver greatly enhances the resilience of GNSS receivers against interference [111]–[113]. Together with applying a high number of bits for quantization or nonlinear quantization, even high-power interference and jammers surpassing an 80 dB interference-to-signal ratio can be suppressed successfully. For military MA receivers, spatial nulling, prewhitening or space-time adaptive processing (STAP) are used for interference and jamming suppression [88], [97]. The number of interference or jamming sources that can be suppressed jointly is dependent on the number of antenna elements. In general, for spatial suppression, only $M - 1$ sources can be suppressed with M antenna elements. For combined space-time processing and STAP approaches, this number can be increased [114], [115]. Recently, it was shown that dual-polarization antenna arrays can also significantly enhance interference and jamming suppression [116], thus introducing multidimensional mitigation.

b: SPOOFING AND MULTIPATHS

The estimation of the direction of arrival (DoA) of all impinging signals combined with attitude determination of the antenna array can be used to detect whether the received signals truly come from GNSS satellites [110]. Thus, spoofing attacks and/or multipaths can be detected and even mitigated by subsequent spatial filtering (beamforming). The application of sophisticated DOA estimation algorithms ensures that spoofing signals can be separated from satellite signals and multipath or other propagation effects. Multiantenna receivers dramatically increase the protection against cyberattacks, especially in repeater attacks, which cannot be detected by authentication methods, and attacks by multiple spoofers (in case the number of spoofers is smaller than the number of in view satellites). On the other hand, as previously mentioned, the introduction of dual-polarization processing provides enhanced multipath mitigation capabilities in some scenarios [33], [117]–[119]. Thus, introducing different domains, i.e., frequency bands, polarization, and correlation (bank of correlators), offers enhanced separation of LOS and multipath signals and consequently improves ranging and positioning performance and robustness. One of these additional domains, of course, is the spatial domain given by an MA receiver.

3) GNSS ARRAY PROCESSING TRENDS

Classic beamforming systems have already shown promising results in earlier years. Hence, MA systems have become the focus of a wider range of applications, especially for SCAps. Interesting approaches using single-polarization antenna arrays have been developed for multipath and joint multipath and interference suppression in recent years [91], [94]–[96]. These multidimensional algorithms, which are often based on maximum likelihood estimation, can also be extended to separate spoofing from multipaths. More recently, array processing algorithms for GNSS that also exploit the polarization domain using a dual-polarization antenna array for multipath mitigation were introduced, e.g., [120]–[122]. To incorporate more domains in the signal processing and to exploit the multidimensional data structure that is provided by GNSSs, tensor-based signal processing approaches were developed, e.g., [90], [93], [103], [123], [124]. These approaches are based on various multidimensional subspace decompositions that enable blind multidimensional filtering or signal component separation with subsequent parameter estimation. These blind algorithms are much less sensitive to array calibration errors, as most of the approaches do not rely on DOA estimation.

Tensor-based approaches have great potential in reducing overall computational complexity, as it is possible for these algorithms to reduce the number of nuisance parameters and thus to enable the design of estimation algorithms that focus on the parameters of interest, i.e., time-delay and carrier phase for GNSSs. These algorithms address the general problem of finding and developing appropriate parameterizations of the signals to achieve the best possible trade-off between computational complexity and estimation accuracy of the parameters of interest and in general have less computational complexity than most multidimensional approaches based on maximum likelihood estimation. They also introduce a general framework to easily include and treat multidimensional data structures consisting of time, frequency bands, correlation, polarization, and spatial domains.

C. HYBRIDIZATION ALGORITHMS

The introduction of MM GNSS receivers in mobile phones and portable devices has raised a myriad of possible working conditions, such as outdoors or indoors, in sparsely populated areas or in deep urban scenarios. Under such conditions, robustness is critical for localization purposes. The main problem in urban scenarios is multipath propagation and the lack of visibility with satellites. This limits the application of HA services such as RTK or PPP. Multipath mitigation and detection techniques can be used to reduce the effects of multipaths. Nevertheless, these techniques may be complex for some MM receivers (as MA techniques are usually too bulky for MM), and they usually lead to a reduction in the available satellites (due to exclusion).

For this reason, the fusion of GNSS with cellular networks or relative positioning technologies, such as radars, SoO, cameras and inertial sensors, is typically considered in constrained environments [15]. These hybrid technologies aim to complement and enhance GNSSs, especially for critical situations with a lack of satellite visibility, such as in tunnels and urban canyons. In this section, we consider integration with INSs based on various sensors, hybridization with 5G communications and hybridization with other SoOs.

1) GNSS/INS HYBRIDIZATION

Inertial sensors can be used to enhance positioning solutions and bridge GNSS outages, significantly increasing accuracy, availability, and robustness. In particular, INSs exploit self-contained IMUs to sense variation in the body position and orientation of a platform [11]. In an IMU, the angular motion is sensed with gyroscopes [125], and the specific force is sensed with accelerometers [126]. In terms of hybridization algorithms, there is a range of integration levels that combine GNSS and INS measurements, and the terminology is not always consistent between publications. In this document, we follow the definitions outlined in [127], and we classify the different integration strategies as *Loose*, *Tight* and *Ultra-tight*, denoting different levels of integration.

The lowest level of integration is *loose integration*. In this approach, the PVT computed from the GNSS receiver is used to correct the INS solution. Then, *tight integration* goes one level beyond by using the GNSS receiver observables to correct the INS. This integration level is beneficial when GNSS visibility is reduced (< 4 satellites) since the integration can still provide some benefit in reducing the INS drift. It is important to note that in these two levels of integration, the INS is not used in any way to check or improve the quality of the GNSS measurement. The highest level of integration, which is useful to improve GNSS, is *ultratight integration*. Here, the GNSS tracking loop uses all available navigation information to track the GNSS signals. This results in a further improvement in the robustness to interference, multipaths, dynamics, lower noise, and faster reacquisition.

It should be emphasized that only MEMS IMUs have size, weight and power (SWaP) parameters compatible with MM, but standalone navigation with MEMS IMUs (i.e., without exploiting a specific motion pattern such as walking) is stable only over a few dozens of seconds. Navigation-grade IMUs employing laser gyros are incompatible with the MM in terms of SWaP but are used for the professional market. One important trend in INS technology worth mentioning is quantum technology-based INS [128]. While quantum sensors may bring fundamental improvements in terms of miniaturization, continuity, and accuracy of the device (as shown by recent developments [129]), the reality is that quantum INSs are still in a relatively early development phase [128], so it may take some time until the technology is used for hybridization with GNSSs.

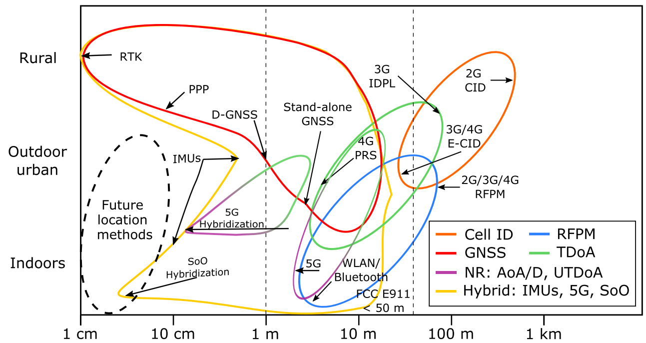

FIGURE 9. Expected horizontal accuracy of GNSS and cellular localization methods for indoor and outdoor scenarios. Hybrid solutions with IMUs, 5G and SoO are also considered.

2) HYBRIDIZATION WITH SIGNALS OF OPPORTUNITY

Hybridization with INSs may be costly and very power-consuming for many applications in MMs. A cheaper and less consuming solution is found with hybridization with SoO from terrestrial communications. These signals are called SoOs because they are designed with purposes other than positioning, but we take the opportunity to use them as such. In this sense, WiFi is currently commonly available in public and in many buildings, which makes it one of the most promising indoor and even outdoor positioning methods with SoO. Most commercially available products using WiFi currently apply received signal strength (RSS) measurements for positioning [130], and they compute the position via Cell-ID, trilateration, and fingerprinting [130]. On the other hand, Bluetooth is the most popular system among the available short-range communications systems. Similar approaches to WiFi are used [131], and combinations of Bluetooth and WiFi positioning are also available in practice for indoor environments [132].

Several products already exist to enable Bluetooth positioning for indoor scenarios, e.g., from InSoft GmbH [133], POLE STAR [134], and Teldio [135]. Other short-range communication systems that are used for positioning are ZigBee, ultrawide-band (UWB), RF identification, and nearfield communication. All these systems can be used for coarse and even more precise positioning. The expected accuracy of positioning of GNSS and SoO can be seen in Fig. 9. One can clearly observe that GNSS positioning can benefit from hybridization with different SoOs in urban and indoor scenarios. Wifi (or WLAN) and Bluetooth already provide very good accuracy in these scenarios based on RSS and trilateration and seem to be very good candidates for hybridization with GNSSs. On the other hand, Cell-ID methods do not seem to improve the accuracy of hybrid solutions with GNSSs.

Hybridization with UWB and similar terrestrial range-based technologies has been shown to be promising for GNSS hybridization [136], [137]. Indeed, there are current technologies for UWB [138] and terrestrial location methods [139] that have already demonstrated indoor accuracies at the centimeter-to-decimeter level. Beyond the traditional SoO mentioned above, another option would be hybridization with communication signals from mega-constellations of satellites in low-earth orbits (LEOs) [140]. In the coming decade, this SoO will be available in large numbers globally [141]. Indeed, LEO-based positioning systems could be considered in the future [142].

3) HYBRIDIZATION WITH 5G

The use of SoO from terrestrial communication systems is of special interest to provide additional ranging measurements for trilateration in GNSSs. However, the lack of information from these terrestrial transmitters, such as the transmitter position or the transmission time, may prevent HA and reliable positioning. This is why cellular networks are preferred for use in navigation fusion. We consider in this section hybridization with 5G, which is expected to play a key role in hybridization solutions over the next decade [15]. Indeed, the combination of GNSSs and cellular networks has attracted special attention along the different network generations [143].

Cellular systems are typically considered to complement the lack of GNSS visibility in urban environments, as discussed in [144]. Unfortunately, due to the limited position accuracy of cellular networks in the first generations (e.g., Cell ID or RF pattern matching, RFPM, see Fig. 9), network providers have usually avoided the costs due to the added complexity of cellular location networks. It was not until the current fourth generation (4G) that dedicated pilots were standardized for positioning [145]. However, disruptive technologies considered in future fifth-generation (5G) networks are envisaged to considerably enhance achievable cellular-based localization [146] due to their inherent HA positioning requirements [147]. Next, three different levels of hybridization are considered based on the works in [79], [143], and [148].

a: SIGNAL-LEVEL HYBRIDIZATION

To date, the synergies between GNSSs and cellular technologies (in terms of localization) have been very limited because their design purposes are very different. However, the demand for a wide range of positioning services has led to a new paradigm in which flexibility is a key asset. The solution adopted in 5G consists of the usage of multicarrier signals with scalable configurations [149], [150]. Therefore, an exploratory concept would be for future GNSS signals to converge to a multicarrier solution as well, thus converging with future 5G networks. The hybridization in this case, understood as the provided added value to GNSSs, is beyond the gains in accuracy and availability that multiple carriers might bring to GNSSs, as shown for 5G positioning methods in Fig. 9. The use of a multicarrier signal for GNSSs would allow quicker convergence to 5G hybridization at all its levels. The reason is that receiver manufacturers could use the same module to process both GNSS and 5G signals, thus simplifying the development of hybrid receivers.

b: PVT-LEVEL HYBRIDIZATION

The hybridization of GNSSs and 5G positioning is a promising research topic that until now has been hindered mainly by the limited knowledge of the transmitted signals (i.e., their location and synchronization) [143], [151]. This limitation has discouraged GNSS hybridization with terrestrial communications. Nonetheless, this trend is expected to change in 5G with the deployment of dedicated positioning services [152]. This opens new opportunities for the hybridization of GNSS and 5G positioning. This is illustrated in Fig. 9, showing positioning capabilities for 5G with an accuracy in the range of [3 - 20] m in scenarios ranging from light-indoor to outdoor/semirural. Another indication in this figure is that the expected accuracy with 5G hybridization ranges from [10 cm - 5 m] for outdoor urban environments.

The main concept of PVT-level hybridization is to combine GNSS observables with 5G observables. However, based on a performance analysis carried out in [79], there is a limited positioning improvement of 5G observables due to the dominant NLOS propagation conditions. Therefore, knowledge of these NLOS conditions is critical to perform adequate weighting within the positioning algorithm. Indeed, there are several solutions to performing NLOS detection and eliminating NLOS paths in 5G [153], [154]. Therefore, in summary, we know that 5G signals help to obtain full availability with hybridization. This is due to the expected high density of 5G base stations in urban environments, which makes the probability of NLOS small, thus facilitating its detection. These capabilities show the usefulness of 5G hybridization to improve the performance of both GNSS and 5G positioning in urban environments, as indicated in Fig. 9.

c: DATA-LEVEL HYBRIDIZATION

The use of cellular networks to assist GNSS receivers has been widely adopted since their introduction in the late 1990s with assisted GPS in 2G networks [143]. An assisted GNSS (A-GNSS) is mainly used to speed up the acquisition and position fixation of MM receivers. This is achieved by using the cellular communication link to transmit to the mobile device the GNSS navigation message (e.g., almanac and ephemeris); otherwise, the mobile device has to demodulate through the GNSS satellite link delaying the time-to-first-fix (TTFF) [39]. Today, new assistance mechanisms could be adopted with 5G to achieve HA and reliable GNSS localization.

Precise GNSS localization can be obtained by means of RTK or PPP [11], which requires a communication link to obtain the differential and precise corrections that allow HA localization. This information could be broadcast (through the 5G network). Therefore, the advantages that can bring data-level hybridization are given in the form of *assisted data* or *corrections*. The former provides a significant reduction in TTFF, a reduced battery consumption, and a high sensitivity (being able to acquire GNSS signals with 25 dB of attenuation with respect to nominal power values) [39]. On the other hand, differential or precise corrections can be used to improve the accuracy. As seen in Fig. 9, RTK and PPP can obtain accuracies as small as 1 cm and 10 cm, respectively. As a drawback, there is an increase in complexity on the receiver side due to having a communication module and the inherent complexity of the RTK or PPP algorithms, but this is the price to pay to obtain the HA positioning given by these methods.

IV. RECEIVER EVOLUTION

The widespread deployment of GNSSs is pushing the current receiver technology to its limits due to the stringent demands to provide seamless, ubiquitous and secure/reliable positioning. This fact is further aggravated by the advent of new applications in which the miniaturized size, LP consumption and limited computational capabilities of user terminals pose serious concerns to the implementation of even the most basic GNSS signal processing tasks. Moreover, the processing of future GNSS receivers is expected to increase due to several factors.

First, an increase in available GNSS signals will be experienced in the coming years. The increasing availability of future signals will have two effects, namely, using more complex modulations and more complex channel coding schemes than those used in legacy signals (e.g., GPS L1C/A). New signal modulations are expected to come in the form of multiplexed BOC signals. For instance, the current Galileo E1-B/C signal is based on a combination of two BOC signals, the so-called CBOC [155]. On the other hand, we have the GPS L1C signal that multiplexes different BOC signals in time [155]. Finally, another example is the current Galileo E5 signal or the future Beidou B2 signal, which are based on the so-called AltBOC modulation [156]. This can increase receiver complexity, but this is aggravated with the new channel coding schemes expected to be employed for future GNSS signal designs. Examples include the low-density parity-check (LDPC) and the Bose-Chaudhuri-Hocquenghem (BCH) codes employed in the GPS L1C [157]. In addition to the abovementioned channel coding schemes, more complex schemes such as Reed-Solomon can be expected, as for the case of the Galileo E6 high accuracy service (HAS) signal [84].

The second reason why the processing complexity of future GNSS receivers is expected to increase is the use of augmentation systems or HA positioning such as RTK or PPP for the MM. Finally, additional processing is needed for authentication, security and integrity issues, such as protecting the position fix from being affected by interferences and abnormal propagation effects [158]. In parallel, emerging GNSS-based applications are gradually extending their operational range by targeting more challenging scenarios, such as urban or light-indoor scenarios. For the case of GNSS, this is forcing user terminals to move outside of their comfort clear-sky zone and to operate in working conditions beyond the limits of their original designs. As a result, serious difficulties have been experienced regarding the availability and accuracy of the GNSS position fix [159]. However, GNSS receivers are extremely power hungry. In fact, it has been stated that continuous GPS tracking can deplete a 1000 mAh battery in only 6 hours [160].

Based on the previous concerns, the GNSS user segment is evolving to more flexible, LP- and SW-based architectures. This evolution has been mainly driven by the use of so-called SW receivers used to process the GNSS signal for different tasks [161]. In the next decade, the use of SW receivers is expected to increase thanks to the development of cloud-based and snapshot solutions [15]. In this section, we provide a comprehensive perspective in terms of the technological evolution of GNSS receivers. In particular, Section IV-A addresses the evolution of SW receivers. Then, Section IV-B and Section IV-C consider the two solutions that are expected to play a predominant role in the GNSS receiver evolution for the next decade. These are cloud-based and snapshot solutions, respectively.

A. SOFTWARE RECEIVERS

As discussed in Section II-C1, ASICs have been the selected choice for baseband processing within a GNSS receiver. Notwithstanding, additional alternatives can be found for GNSS signal processing, such as CPUs, FPGAs, DSPs, and GPUs. As these elements can be programmed with different programming languages (e.g., C/C++, Python, Java/avaScript, ...), the resulting receivers are called SW-defined radio, SDR (mostly if CPUs or DSPs are involved) or SW receivers (for FPGAs) [161]. The scientific community has taken advantage of the features of the GPUs to perform simulations [162], but the use of GPUs for GNSS signal processing is still quite limited, as the replica generation and correlation operation is intrinsically serial and not well suited for parallelization. Furthermore, communications between CPUs and GPUs cause a significant overhead that impact processing in general-purpose receivers [163].

The main use of SW receivers is postprocessing, which allows researchers to test new algorithms and adjust the receiver to the application case. The receiver can also be reprogrammed at any time to add new features such as the processing of future signals (e.g., L1C) and new applications. The receiver design has three main tasks: signal acquisition, tracking, and position computation based on the obtained ranging information (see Fig. 1). For acquisition, FFT/IFFT algorithms can be employed (here, the GPU provides a significant performance gain). For tracking, tracking loops are used in which the correlation between the incoming signal and the locally generated replica is determined. However, the required power consumption of an SW receiver is too high (as of a study presented in [164] in 2015, an embedded software receiver required between 2.5 and 4.5 W, the study also provides an evolution trend for embedded software receivers) in comparison to the low mW required by ASIC receivers.

In conclusion, SW receivers are very flexible tools capable of implementing several different configurations and features for various GNSS applications. However, they require an RF-FE that down-converts and digitizes the GNSS signals. This makes the whole system bulky and expensive. This implies the continued use of ASIC receivers in future market GNSS receivers. The RF-FE is also required for ASICs, however, the whole system is still much smaller when compared with whole SW receiver systems. Real-life applications for SW receivers are possibly autonomous cars, in which data from many sensors are mixed with GNSS signals (i.e., deep GNSS/INS) or in critical infrastructure applications with large enough platforms in which the latest signals and features of GNSS can be easily implemented in the receivers. Actually, the use of SW receivers is expected to increase in the future thanks to the advent of cloud-based and snapshot solutions, both considered in the following sections.

B. CLOUD-BASED SOLUTIONS

Based on the demands of GNSS technological evolution and the new era of applications, cloud computing has become an exceptional opportunity to migrate GNSS signal processing tasks into a scalable, distributed and high-performance computing platform [165]–[167]. Cloud-GNSS processing has been sparsely considered in the literature [19], [168]–[172]. In this section, we provide a general perspective of cloud-GNSS receivers with the aim of combining the key aspects currently spread throughout the literature. Specifically, we first introduce the architecture of a conventional GNSS sensor, followed by a description of the general architecture of a cloud-GNSS receiver. Finally, we compare the performance of both traditional and cloud-based GNSS processing so that its feasibility in terms of energy consumption, PVT accuracy and economic cost is evaluated.

1) CONVENTIONAL GNSS SENSOR

The basic architecture of a conventional positioning sensor is the traditional architecture shown in Fig. 1, which is in charge of gathering, digitizing, acquiring, and tracking the GNSS signal. Furthermore, in addition to the GNSS module, any positioning sensor is composed of other components in charge of the power supply, memory, communications and processing control. All these elements are shown in Fig. 10. As described in the figure, the GNSS sensor, beyond capturing, digitizing and processing the GNSS signal, generates an output (usually an NMEA file) that is stored in memory or delivered to a remote-control center for further processing.

Therefore, in a conventional approach, sensors obtain their position (among other GNSS and localization information) and transfer the results to a remote server or store it in memory for eventual processing. One important aspect for the comparison with a cloud-based receiver is the energy consumption of a conventional GNSS sensor. As already analyzed and discussed in this paper, the most energy-consuming component of a GNSS sensor is the GNSS module, particularly during the

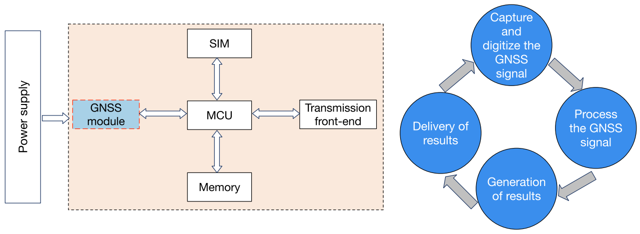

FIGURE 10. Architecture and workflow of a conventional GNSS sensor.

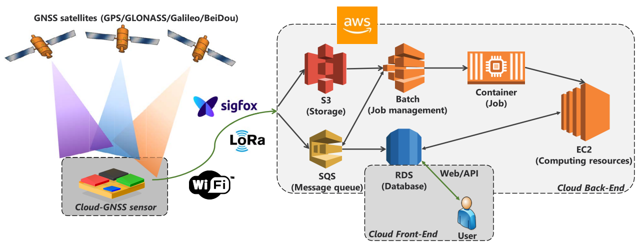

FIGURE 11. Example of a cloud GNSS receiver architecture.

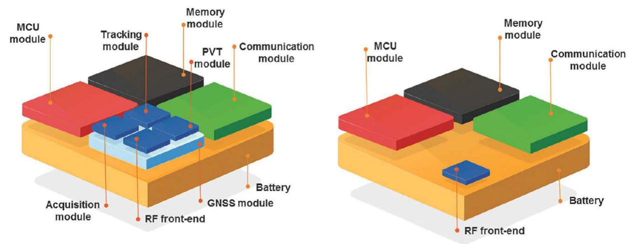

FIGURE 12. Comparison between a conventional GNSS sensor (left) and cloud-based GNSS sensor (right) [19].

acquisition stage. Further details on the energy consumption of a conventional GNSS sensor and its comparison with a cloud-based solution are given in Section IV-B3.

2) CLOUD-GNSS RECEIVER ARCHITECTURE

The ultimate goal of a cloud-GNSS receiver is to reduce the power consumption without compromising the accuracy. From a system perspective, a cloud-GNSS receiver is composed of three main elements interconnected as in Fig. 11: the *cloud-GNSS sensor* or user terminal, the *cloud front-end module* in charge of interacting with the user (Web/API), and the *back-end module* in which the GNSS SW receiver is actually running. All these elements of the cloud architecture are indicated in Fig. 11.

The *cloud-GNSS sensor* is in charge of gathering the GNSS samples at the user side and sending them to the cloud for subsequent processing. The main difference from a traditional GNSS sensor is shown in Fig. 12, which is the presence of the GNSS module in the traditional sensor. This module is the most energy-consuming module in a GNSS sensor, which is why the cloud-GNSS sensor is designed (see right plot of Fig. 12) to gather, digitize the GNSS signal and transfer this information to a cloud server. This is in contrast to a traditional sensor, which has to locally process the GNSS data. Currently, cloud-GNSS sensors can be built by means of SDR products (see [169]). In the near future, however, IoT sensors are expected to be miniaturized with LP consumption, thus leading to cheaper, smaller and more efficient GNSS sensors.

From a service point of view, the cloud-GNSS receiver is a remote application configurable by the user to obtain some output results. The first platform providing these kinds of services was Amazon web services (AWS). Today, there is a wide spectrum of options for cloud computing, such as the Google cloud platform, Microsoft Azure, RedHat Openshift, or Oracle cloud. Access to these services is provided by the *cloud front end*, which is the interface through which a user or a machine interacts with the cloud-GNSS receiver [19]. The main task of the cloud front end is to generate a new job in the cloud-GNSS receiver with a raw GNSS sample and a JavaScript Object Nation (JSON) configuration file as input. Then, the files and job instructions generated by the cloud front end are transferred to the *cloud back end*, which is in charge of the processing task to be carried out. This includes processing the GNSS raw samples but also generating the output reports to be delivered to the user.

3) PERFORMANCE ANALYSIS

In this section, we analyze the cloud-GNSS paradigm and its feasibility in terms of energy consumption and economic cost. We also compare these results with those obtained with traditional positioning. We follow the analysis performed in [19].

a: ENERGY CONSUMPTION

To compare the energy consumption of a traditional and cloud-GNSS receiver, we consider the analysis performed in [19] for state-of-the-art commercial components. Different start conditions are considered to cover all the umbrellas of commercial receivers. These conditions are measured by the so-called TTFF of the GNSS module, which fixes the time in active mode of the module. The energy consumption of the different modes is shown in Fig. 13 with a comparison of cloud-based receiver consumption as a function of the signal length to be processed. The results in dashed lines show that the energy consumption of the GNSS module depends on the operation mode (i.e., hot, assisted, warm, cold) and hence strongly depends on the TTFF.

Indeed, compared to a conventional sensor with the lowest consumption mode (i.e., hot start), the cloud sensor is more energy efficient when using a signal length of up to 24 ms. For the most consuming modes (i.e. warm and cold starts), the cloud-GNSS sensor can remain active for hundreds of milliseconds (up to 600 and 800 ms, respectively) and is still more energy efficient. Thus, the energy efficiency of cloud-based solutions ranges from 1 to 2.5 orders of magnitude. It is important to bear in mind that a PVT can be obtained with just a few ms of signal (depending on the GNSS

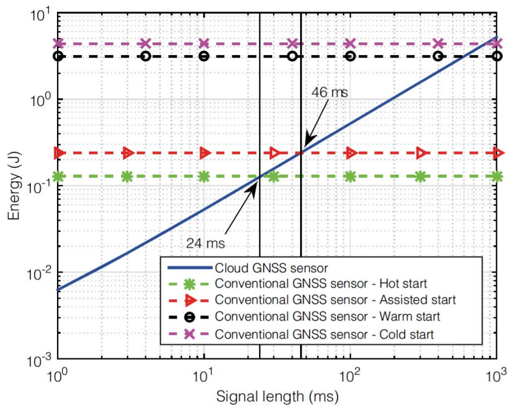

FIGURE 13. Expected energy consumption of a cloud and a conventional GNSS sensor as a function of the signal length [19].

signal). Therefore, the user of a cloud-GNSS receiver has to face a trade-off between the signal length and the given accuracy and sensitivity. The reason is that as the signal length increases, so does the energy consumption, but at the same time, the sensitivity and accuracy are also increased and vice versa.

b: PVT ACCURACY

Next, we briefly discuss the accuracy performance of the cloud-GNSS receiver by means of an experimental test published in [19]. The obtained results for GPS L1 C/A conclude that for a small signal length (i.e., 1 to 4 ms), a position error of tens of meters is obtained with a cloud-GNSS receiver. However, as the coherent integration time is increased (i.e., 10 and 20 ms), and hence the amount of signal captured and sent to the cloud-GNSS receiver is also larger, the positioning accuracy is enhanced to a few meters. In contrast to conventional GNSS IoT positioning approaches in which the sensor must be in active mode for a long period of time to calculate the PVT (from a few seconds up to minutes, depending on the working conditions), in a cloud-based approach, the sensor must be in active mode for just a few ms, which is enough time to capture the desired GNSS signal, forward it to the cloud and obtain a PVT solution with enough accuracy.

c: ECONOMIC COST

Processing the raw GNSS sample file in cloud servers instead of in the sensor itself, as in conventional approaches, implies the added cost of hiring cloud computing resources. For instance, AWS offers three different types of services (on-demand, reserved and spot) with three different fees. For the analysis, we consider a cloud back-end with 4 CPUs, 1.5 GB of RAM memory, and 2 solid-state drives with 40 GB. Furthermore, we consider three different prices (without taxes) for AWS: 0.258, 0.11 and 0.0472 $/hour. Finally, we consider a signal length between 1 and 5 ms, which is enough to process some GPS and Galileo signals. With this setting, the monthly cost of the necessary cloud resources for an IoT application that requires one position fix per hour is $0.51, $0.23 and $0.1 per month for the different services, respectively. Note that in typical IoT positioning applications, a position fix is usually requested from hours up to days. In terms of chip cost, cloud-based GNSS receivers are, in principle, expected to be cheaper than traditional GNSS receivers, as the chip no longer requires a CPU for PVT computation and ASIC for baseband processing.

C. SNAPSHOT SOLUTIONS

One of the main concerns of MM receiver manufacturers is the power management of the GNSS sensor. We know today that receivers are extremely power hungry, so new LP architectures must be sought. In particular, user segment technologies embraced under the umbrella of snapshot, open-loop or HS GNSS techniques are able to circumvent these hurdles to some extent. All this terminology is used across the GNSS literature [8], [159], [160], [173], [174], but we collect them together in this section as a new receiver evolution, namely, snapshot solutions. These solutions are designed to work with only a few milliseconds of raw GNSS signals, defined as snapshots. Snapshots are then passed to the host platform processor (e.g., an SW receiver), stored for later processing (e.g., a GNSS sensor/tracker) or sent to the cloud. This approach is specifically designed for scenarios when continuous tracking is not possible (e.g., indoors), not required (e.g., on-demand PVT) or not desirable (e.g., LP consumption) [173]. Several practical examples can be found in commercially available products [175]–[177]. The clearest examples of modern devices implementing snapshot processing are current smartphones or cloud-based solutions, which are closely related to snapshot processing.

In summary, snapshot positioning targets two different configurations for the snapshot length. The options are a relatively large snapshot (greater than 100 ms) or a short snapshot configuration (as little as 2 ms) [173]. The former is aimed for HS solutions, whereas the latter is intended for LP solutions. In comparison, a conventional GNSS receiver may require a few to tens of seconds of signal tracking before it is able to compute its first position. In the following, we describe the operating modes of snapshot receivers that allow manufacturers to design HS or LP GNSS receivers based on snapshot techniques. Then, the two following sections are aimed at analyzing their specific evolution for HS and LP solutions. Finally, we show some practical results of snapshot positioning.

1) SNAPSHOT RECEIVERS

One very unique feature of snapshot receivers is their flexibility to reconfigure and initiate the three logical blocks of a GNSS receiver (see Fig. 1) on and off the receiver device. For instance, for use cases in which maximizing battery life is more critical than real-time positioning, the snapshot receiver can be configured such that only the signal capture circuitry is implemented to temporarily store the digital samples. Signal processing is postponed until such a time that the digital

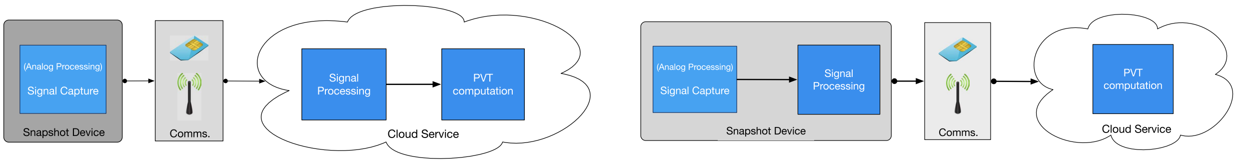

FIGURE 14. Flexibility of a snapshot receiver: (Left) Only performing signal capture on the device and signal processing + PVT computation performed in a remote server. (Right) Signal capture and processing implemented on the device.

samples can be transmitted, without affecting the battery life of the device (e.g., during battery recharge), to a remote cloud server for the rest of the GNSS signal processing. This is illustrated in the left plot of Fig. 14, and it is the same concept used in the most energy efficient mode of the product in [175]. In this mode, the snapshot receiver can operate up to several weeks on a single coin cell battery or years on a typical mobile phone battery.

On the other hand, for use cases in which position information is needed at the device (real-time applications), the snapshot receiver can be configured such that all the blocks are implemented on a single circuitry, such as the setup used in [176]. This is similar to traditional GNSSs but with some ad hoc techniques to obtain HS or LP. Finally, the right plot of Fig. 14 shows a hybrid architecture in which the snapshot receiver is configured to gather the signal samples and then to generate measurements prior to transmitting them to the remote server for the ultimate position computation. The alternate mode for the real-time application of [175] fits with this architecture. Therefore, in general, state-of-the-art snapshot receivers offer system designers considerable flexibility to tailor an LP and low-cost GNSS solution that is most suitable for their HW implementation and use cases.

2) HIGH-SENSITIVITY (HS) PROCESSING

The excellent performance provided by GNSSs in outdoor environments is attracting interest in extending their applications to harsher environments, such as urban canyons, inside building and forested areas. As already mentioned, in these environments, the acquisition and tracking of a GNSS signal is challenging. This fact has led to the development of HS techniques for GNSS receivers. They usually deal with acquiring weak signals by coherently accumulating signal samples for a long period of time (i.e., the coherent integration time T_{coh}). However, there are two key factors that limit the maximum integration time, and they bound the minimum detectable SNR. On the one hand, the presence of unknown data bit transitions introduces sign reversals within the integration window, which may cause a partial or even total cancellation of the correlation power. To overcome this issue, noncoherent accumulations can be performed, but then the T_{coh} will be limited by the bit length. On the other hand, as already noted, the quality of the user receiver clock limits T_{coh}.

The issue of the presence of bit transitions has already been addressed by the incorporation of pilot components in

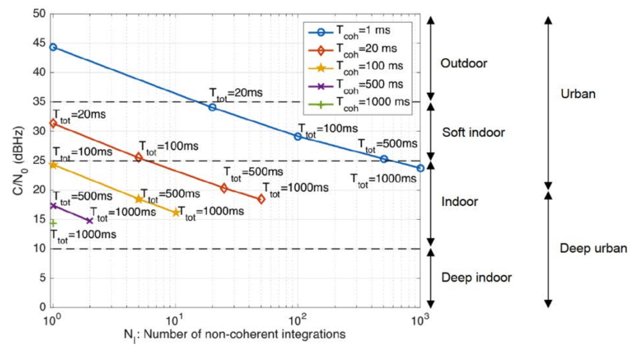

FIGURE 15. Minimum detectable CN0 (i.e., sensitivity) for a Galileo E1C signal using a 4 MHz front end targeting a 90% probability of detection and 1E-4 probability of false alarm.

Galileo signals, and this has been proven to be a major facilitator for the operation of GNSS receivers under weak signal conditions. However, regarding the receiver clock oscillator stability, this is a feature in which receiver manufacturers will need to work to improve the performance and reduce costs. Currently, the most widely adopted clocks are TCXO and OCXO, which are typically used in MM and professional applications, respectively, with up to 100 ms coherent integration with TCXO and up to 1000 ms coherent integration with OCXO [178]. This is an important factor impacting the sensitivity of a GNSS receiver. This point is shown in Fig. 15, which illustrates the minimum detectable CN0 of an example of GNSS receiver processing the Galileo E1C signal. With the analysis of this figure, we see nearly a 10 dB gain in terms of sensitivity for an OCXO clock compared to a TXCO. Unfortunately, the cost of OCXO clocks is still much higher than that of TCXO clocks, thus preventing the former from being widely adopted in MM GNSS receivers.

3) LOW-POWER (LP) PROCESSING

As discussed, the main drawback of employing a GNSS module to obtain the PVT solution in an IoT sensor is the cost and power consumption, typically being one the most power-hungry devices of the whole sensor, thus significantly reducing the battery life. Together with the use of novel semiconductor technologies, MM GNSS vendors are addressing the power consumption quandary with three different alternatives, namely, the *efficient processing load*, the *use of A-GNSS*, and *duty cycle operations*. The former is intended to select a subset from all the visible satellites, maintaining similar performance as using the whole set of satellites. To do so, most of the approaches are focused on minimizing the GDOP [179], [180]. More sophisticated methods perform a selection based both on the geometry and measurement errors [33], [181]. For instance, [33] used a dual-polarized antenna to exclude the NLOS measurements from the PVT computation. The results show great improvements in the accuracy, particularly in urban scenarios, reducing the errors up to 50% of the errors without excluding measurements.

Regarding the use of *A-GNSS*, we have to consider that a key parameter of any GNSS receiver is the TTFF. For instance, to decode the navigation message of a GPS L1 C/A signal, a GNSS receiver requires a minimum of 30 s of signal. A TTFF with a minimum of 30 s is prohibitive in LP positioning. To reduce that TTFF, current GNSS receivers download A-GNSS data, which greatly reduces the amount of signal needed to obtain a first fix to milliseconds [174]. Finally, *duty cycle* operations diminish the average power consumption of a GNSS module, as most components are shut down (i.e., sleep) between position fixes [177]. Nonetheless, duty cycle configurations have been shown to degrade the accuracy of the PVT solution, being worse for longer sleep states [49], [182]. The most common duty cycle operations found in the literature are (i) noncontinuous block tracking, as described in some Broadcom patents [183], [184], and (ii) duty-cycle tracking, in which the tracking only operates for a fraction of time [185], [186].

4) PERFORMANCE ANALYSIS

Based on the study in [174], we provide here a summary of the accuracy performance we can obtain with a snapshot receiver. First, the accuracy of the snapshot receiver in a hot start is slightly degraded whenever the duty cycle operation mode is used instead of the continuous mode. However, when the receivers are configured with a cold start, duty cycle operation modes significantly disrupt the performance, up to the limit of not being able to provide any position fix during the whole test (i.e., 10 minutes), whereas the obtained availability with continuous mode is 90%. On the other hand, a cloud-based snapshot GNSS receiver offers full availability for both signal lengths of 20 and 1000 ms. Furthermore, the obtained accuracy within 20 ms is larger than that obtained by the GNSS receivers in continuous mode.

V. CONCLUSION

Next, we conclude the paper by giving a perspective on GNSS technology evolution, a list of current GNSS chipsets and a summary of the concluding remarks.

A. PERSPECTIVE OF GNSS TECHNOLOGY

Apart from the HW evolution described in this paper, which will drive future GNSS receivers to be smaller, cheaper, more powerful, and less power hungry, two main trends are identified that will drive the user technology evolution in the years to come: robustness against jamming, multipaths, and spoofing as well as LP consumption techniques. Based on the perspective provided in this paper, the main drivers for the evolution of GNSS user technology are as follows:

- From the HW point of view, higher diversity receivers are expected in terms of available frequency bands as a function of the application requirement. A clear example is given with the single-frequency E5/L5 Sony receiver, while multifrequency receivers are expected to become more popular in MM receivers. The receiver type is still expected to employ ASIC technology, as it is currently the most cost-efficient technology for MM receivers. Equivalently, most oscillators in MM receivers will continue to be crystal oscillators unless high accuracy is required, in which a proliferation of TCXO oscillators is expected.
- From the PVT perspective, the availability of a higher number of signals and frequencies will allow a higher accuracy in required applications. Additionally, the future availability of authentication, e.g., provided by Galileo OSNMA, will allow higher receiver robustness against spoofing. The first ones to benefit from such capability are expected to be the more complex receivers, such as SCAp or professional receivers. However, more complex PVT algorithms are not feasible for LP receivers due to the computational complexity, which is translated into a higher implementation costs and increased power consumption for a small improvement in the computed position accuracy. This statement is also applied to the digital processing stage, when the implementation of the processing of the whole signal bandwidth is applied (e.g., including the BOC(6,1) for Galileo E1-B/C) in a receiver.
- Receivers will evolve to be more robust with high levels of integrity. This is expected to be achieved thanks to the use of MA and hybrid solutions as well as the broader application of MC and MA receivers. This will provide more secure and professional applications based on GNSSs.
- In parallel, MM receivers are expected to evolve into LP and more accurate solutions. This will be due to the proliferation of cloud-based, snapshot and hybrid solutions, allowing more accurate solutions with LP consumption to a wider range of users than is possible today.

Cloud-based, MA, hybrid, and snapshot solutions are the solutions identified in this paper to evolve GNSS technology from an architectural point of view. From a market point of view, Table 3 illustrates the mapping between the considered solutions and the different segments, as defined in the GSA user technology report [15]. The table shows the likelihood of each solution to be applied in each segment to improve the corresponding key performance. The likelihood is measured as high (✓), medium (∼) and low (✗), based on the perspective provided in this paper.

TABLE 3. Matrix with the mapping between the solutions proposed in this document and the GSA user technology report.

		Considered Solutions			
		Cloud-based	Multi-antenna	Hybrid	Snapshot
GSA User Technology Report	MM segment Low-power High-accuracy	✓	✗	∼	✓
	SCAp segment Integrity Robustness	∼	✓	✓	✗
	Professional segment High-accuracy Integrity	✗	✓	✓	✓

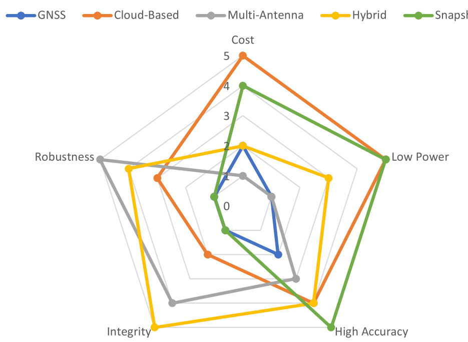

FIGURE 16. Main future challenges and solutions in GNSSs compared to traditional GNSSs. A ratio from 1 to 5 is given to each solution for every key performance indicator (KPI), and it is compared with traditional GNSSs.

Hence, we expect the following impact: cloud-based and snapshot solutions will increase the influence on the MM segment to achieve the requirements in terms of LP and HA. MA and hybrid solutions are expected to evolve the SCAp segment in terms of integrity and robustness. Similarly, these two solutions will help the professional segment improve both integrity and accuracy. Furthermore, the professional segment might evolve to more accurate and sensitive solutions with the use of snapshot receivers. This summary is illustrated in the form of a radar-chart diagram in Fig. 16 that compares the impact of the considered solutions on the most relevant key performance indicators (KPIs) in GNSSs with traditional GNSS technology.

B. CURRENT GNSS CHIPSETS IN THE MARKET

This section provides an overview of exemplary and recent GNSS chips but is by far not exhaustive. The analysis shown in Table 4 is performed by selecting a few chips among the most relevant chips and observing their receiver capabilities in terms of RF bands that can be processed and the services able to process (services understood as GNSS and regional system processing capabilities). The availability of processing the four GNSS systems is common for most current chips; therefore, the main difference is provided in the capability of processing the signals from regional systems, such as the Indian NAVIC or the Japanese QSZZ. In addition, it is observed that current chips can process SBAS augmentation signals.

TABLE 4. Current relevant GNSS chips and modules in the market.

GNSS chip/module	Supported bands	Supported services	Targeted market
Sony CXD5610GF/GG [35]	L1/E1/B1 L5/E5a/B2	GPS, Galileo, BeiDou, GLONASS, NAVIC, QSZZ, SBAS	Enhanced accuracy and IoT (MM)
Broadcom BCM47765 [187]	L1/E1/B1 L5/E5a/B2	GPS, Galileo, BeiDou, GLONASS, NAVIC, QSZZ, SBAS	Enhanced accuracy (MM)
U-blox MAX-M10 series [188]	L1/E1/B1	GPS, Galileo, BeiDou, GLONASS, SBAS	IoT (MM)
U-blox ZED-F9P [189]	L1/E1/B1 L5/E5/B2 L2	GPS, Galileo, BeiDou, GLONASS, QZSS, SBAS	High-accuracy with carrier-phase + RTK (Professional)
Qualcomm snapdragon 855 [34]	L1/E1/B1 L5/E5a	GPS, Galileo, BeiDou, GLONASS, QZSS SBAS	Enhanced accuracy (MM)
STA8100GA [190]	L1/E1/B1 L5/E5/B2 L2 E6	GPS, Galileo, BeiDou, GLONASS, NAVIC, QZSS	Automotive

It can be observed that IoT receivers are still expected to be single-frequency receivers. If more accuracy is required, e.g., for smartphones, dual-frequency receivers are available. The targeted market for each receiver presented in Table 4 is provided in the last column in terms of MM, professional and/or SCAp, as indicated by the manufacturers themselves. As observed, the GNSS chip design trend tends towards both enhanced accuracy and LP but with only partial support for PPP or RTK applications. It must be noted that SCAp chipsets are not usually available for the public, as they are available only with complete receiver or receiver modules, including a significant number of discrete electronic components.

C. CONCLUDING REMARKS

In this paper, we have provided a comprehensive overview of the technological trends of GNSS user equipment. We have considered basic HW components to process and receive GNSS signals, including the algorithms running on integrated systems. Application-specific integrated circuits are identified as the main platforms employed for IF or baseband signal processing, and semiconductor evolution is the main trend identified for the further development of receiver HWs. This also comes with a reduction in the energy consumption of the GNSS receiver and provides additional space, which might be used in different ways depending on the application scenario of the receiver, e.g., to provide higher processing power or to increase the available memory for other tasks. On the other hand, GNSS algorithms are evolving towards ubiquitous PPP and high accuracy PVT algorithms. This is achieved by adding carrier phase measurements and by using code measurements from new high-bandwidth GNSS signals, e.g., processing Galileo's E5 signal. Thus, GNSS receiver manufacturers are developing MM receivers implementing PPPs and/or RTKs (as is done today for HA receivers) in an LP manner. This implies that the antennas are the main HW element that differentiates MM and HA receivers. An additional trend has been identified, achieving higher robustness against interference, multipaths, and spoofing by using MA systems. To do so, multiple antennas are used, thus reducing the market impact due to the size, cost, and complexity of these systems. A cheaper and smaller alternative can be found for some applications by the hybridization of GNSSs with other technologies, particularly with 5G communications.

REFERENCES

[1] M. Z. Chowdhury, M. Shahjalal, S. Ahmed, and Y. M. Jang, "6G wireless communication systems: Applications, requirements, technologies, challenges, and research directions," *IEEE Open J. Commun. Soc.*, vol. 1, pp. 957–975, 2020, doi: 10.1109/OJCOMS.2020.3010270.

[2] Q. Luo, Y. Cao, J. Liu, and A. Benslimane, "Localization and navigation in autonomous driving: Threats and countermeasures," *IEEE Wireless Commun.*, vol. 26, no. 4, pp. 38–45, Aug. 2019.

[3] A. Al-Fuqaha, M. Guizani, M. Mohammadi, M. Aledhari, and M. Ayyash, "Internet of Things: A survey on enabling technologies, protocols, and applications," *IEEE Commun. Surveys Tuts.*, vol. 17, no. 4, pp. 2347–2376, 4th Quart., 2015.

[4] J. Neil, L. Cosart, and G. Zampetti, "Precise timing for vehicle navigation in the smart city: An overview," *IEEE Commun. Mag.*, vol. 58, no. 4, pp. 54–59, Apr. 2020.

[5] V. U. Zavorotny, S. Gleason, E. Cardellach, and A. Camps, "Tutorial on remote sensing using GNSS bistatic radar of opportunity," *IEEE Geosci. Remote Sens. Mag.*, vol. 2, no. 4, pp. 48–48, Dec. 2014.

[6] W. Wen, G. Zhang, and L.-T. Hsu, "Object-detection-aided GNSS and its integration with Lidar in highly urbanized areas," *IEEE Intell. Transp. Syst. Mag.*, vol. 12, no. 3, pp. 53–69, 2020.

[7] R. Rodriguez, D. M. Jenkins, J. J. K. Leary, K. M. Nolan, and B. V. Mahnken, "Performance analysis of GNSS units in manned helicopter operations,"*IEEE Aerosp. Electron. Syst. Mag.*, vol. 33, no. 10, pp. 14–20, Oct. 2018, doi: 10.1109/MAES.2018.170125.

[8] G. Seco-Granados, J. A. López-Salcedo, D. Jiménez-Baños, and G. López-Risueño, "Challenges in indoor global navigation satellite systems," *IEEE Signal. Proc. Mag.*, vol. 29, no. 2, pp. 108–131, Mar. 2012.

[9] B. W. Parkinson, P. Enge, P. Axelrad, and J. J. Spilker, *Global Positioning System: Theory Application*. Reston, VI, USA: American Institute of Aeronautics and Astronautics, 1996.

[10] P. Misra and P. Enge, *Global Positioning System: Signals, Measurements and Performance*. Nagpur, India: Ganga-Jamuna, 2012.

[11] P. Teunissen and O. Montenbruck, *Handbook of Global Navigation Satellite*. New York, NY, USA: Springer, 2017.

[12] M. Naruoka, "Application of inertial and GNSS integrated navigation to seabird biologging," *J. Robot. Mechatron.*, vol. 33, pp. 526–536, Jan. 2021.

[13] M. Pini, A. Minetto, A. Vesco, D. Berbecaru, L. M. C. Murillo, P. Nemry, I. De Francesca, B. Rat, and K. Callewaert, "Satellite-derived time for enhanced telecom networks synchronization: The ROOT project," in *Proc. IEEE 8th Int. Workshop Metrol. Aerosp.*, Jun. 2021, pp. 288–293.

[14] E. Falletti, D. Margaria, G. Marucco, B. Motella, M. Nicola, and M. Pini, "Synchronization of critical infrastructures dependent upon GNSS: Current vulnerabilities and protection provided by new signals," *IEEE Syst. J.*, vol. 13, no. 3, pp. 2118–2129, Sep. 2019.

[15] *GNSS User Technology Report*, GSA, Prague, Czech republic, 2020.

[16] K. Lam, "Broadcom introduces world's first dual frequency GNSS receiver with centimeter accuracy for consumer LBS applications," Broadcom, San Jose, CA, USA, Tech. Rep. 21, 2017.

[17] M. Cuntz, A. Konovaltsev, and M. Meurer, "Concepts, development, and validation of multiantenna GNSS receivers for resilient navigation," *Proc. IEEE*, vol. 104, no. 6, pp. 1288–1301, Jun. 2016.

[18] I. Yaqoob, L. U. Khan, S. M. A. Kazmi, M. Imran, N. Guizani, and S. C. Hong, "Autonomous driving cars in smart cities: Recent advances, requirements, and challenges," *IEEE Netw.*, vol. 34, no. 1, pp. 174–181, Jan./Feb. 2020.

[19] V. Lucas-Sabola, G. Seco-Granados, J. A. López-Salcedo, J. A. García-Molina, and G. W. Hein, "GNSS IoT positioning: From conventional sensors to a cloud-based solution," in *Proc. InsideGNSS*, May 2018, pp. 53–62.

[20] Å. Štern and A. Kos, "Positioning performance assessment of geodetic, automotive, and smartphone GNSS receivers in standardized road scenarios," *IEEE Access*, vol. 6, pp. 41410–41428, 2018, doi: 10.1109/ACCESS.2018.2856521.

[21] T. Hassan, A. El-Mowafy, and K. Wang, "A review of system integration and current integrity monitoring methods for positioning in intelligent transport systems," *IET Intell. Transp. Syst.*, vol. 15, no. 1, pp. 43–60, Jan. 2021.

[22] T. S. Tcr, *Robotic Vehicles: Systems and Technology*. Singapore: Springer, 2021.

[23] *GNSS Market Report*, GSA, Prague, Czech Republic, Sep. 2010.

[24] *GNSS Market Report*, GSA, Prague, Czech Republic, Jun. 2019.

[25] *GNSS User Technology Report*, GSA, Prague, Czech Republic, Feb. 2018.

[26] M. Fortunato, J. Critchley-Marrows, M. Siutkowska, M. L. Ivanovici, E. Benedetti, and W. Roberts, "Enabling high accuracy dynamic applications in urban environments using PPP and RTK on Android multi-frequency and multi-GNSS smartphones," in *Proc. Eur. Navigat. Conf. (ENC)*, Apr. 2019, pp. 1–9, doi: 10.1109/EURONAV.2019.8714140.

[27] D. Psychas, S. Verhagen, and P. Teunissen, "Precision analysis of partial ambiguity resolution-enabled PPP using multi-GNSS and multi-frequency signals," *Adv. Space Res.*, vol. 66, no. 9, pp. 2075–2093, 2020.

[28] J. J. H. Wang, "Antennas for global navigation satellite system (GNSS)," *Proc. IEEE*, vol. 100, no. 7, pp. 2349–2355, Jul. 2012.

[29] C. G. Bartone, "GNSS soltuions: Will I need a new antenna for the new GPS and GALILEO signals? Will one antenna work for both systems," in *Proc. InsideGNSS*, Mar./Apr. 2006, pp. 21–23.

[30] B. R. Rao, W. Kunysz, R. Fante, and K. McDonald, *GPS/GNSS Antennas*. Norwood, MA, USA: Artech House, 2013.

[31] W. de Wilde, B. Bougard, J.-M. Sleewaegen, G. Cuypers, A. Popugaev, M. Landmann, C. Schirmer, D. Egea-Roca, J. A. Lopez-Salcedo, and G. Seco-Granados, "Authentication by polarization: A powerful anti-spoofing method," in *Proc. Int. Tech. Meeting Satell. Division The Inst. Navigat.*, Miami, FL, USA, Sep. 2018, pp. 3643–3658.

[32] T. Kraus, F. Ribbehege, and B. Eissfeller, "Use of the signal polarization for anti-jamming and anti-spoofing with a single antenna," in *Proc. ION GNSS*, Tampa, FL, USA, Sep. 2014, pp. 3495–3501.

[33] D. Egea-Roca, A. Tripiana-Caballero, J. López-Salcedo, G. Seco-Granados, W. De Wilde, B. Bougard, J.-M. Sleewaegen, and A. Popugaev, "Design, implementation and validation of a GNSS measurement exclusion and weighting function with a dual polarized antenna," *Sensors*, vol. 18, no. 12, p. 4483, Dec. 2018, doi: 10.3390/s18124483.

[34] Qualcomm. *Qualcomm Snapdragon 855 Mobile Platform*. Accessed: Nov. 24, 2021. [Online]. Available: https://www.qualcomm.com/documents/snapdragon-855-mobile-platform-product-brief

[35] *Sony Releases GNSS Receiver LSIs for IoT and Wearable Devices*, InsideGNSS, Eugene, Oregon, 2020.

[36] G. Turetzky and P. McBurney, "A pure L5 mobile receiver," in *Proc. InsideGNSS*, Sep./Oct. 2020, pp. 40–42.

[37] G.López-Risueño, D. Jiménez-Baños, F. González-Martínez, P. Waller, M. Colina-Farjó, "User clock impact on high sensitivity GNSS receivers," in *Proc. ENC-GNSS*, Toulouse, France, Apr. 2018, pp. 1–9.

[38] SiTime Products. *SiTime SiT5155±0.5 PPM, Elite Platform Super-TCXO for GNSS/GPS*. Accessed: Nov. 24, 2021. [Online]. Available: https://www.sitime.com/products/super-tcxos/sit5155

[39] F. V. Diggelen, *A-GPS Assisted GPS, GNSS, and SBAS*. Norwood, MA, USA: Artech House, 2009.

[40] J. O. Winkel, "Modeling and simulating GNSS signal structures and receivers," Ph.D. dissertation, Dept. Civil Eng. Surv., Univ. Federal Armed Forces Munich, Neubiberg, Germany, 2000.

[41] D. Calero, E. Fernandez, and M. E. Pares, "Positioning performance of chip-scale atomic clock GNSS augmentation systems," in *Proc. 8th ESA Workshop Satell. Navigat. Technol. Eur. Workshop GNSS Signals Signal Process. (NAVITEC)*, Dec. 2016, pp. 1–7, doi: 10.1109/NAVITEC.2016.7849326.
[42] R. Ramlall, J. Streeter, and J. F. Schnecker, "Three satellite navigation in an urban canyon using a chip-scale atomic clock," in *Proc. ION GNSS*, 2011, pp. 2937–2945.
[43] S. Preston and D. Bevly, "CSAC-Aided GPS multipath mitigation," in *Proc. 46th Annu. Precise Time Interval Syst. Appl. Meeting*, 2016, pp. 228–234.
[44] M. Petovello, D. H. Olesen, J. Jakobsen, and P. Knudsen, "Are there low-cost and low-weight options for GNSS IF storage," in *Proc. InsideGNSS*, Sep./Oct. 2016, pp. 40–45.
[45] F. Bastide, D. Akos, C. Macabiau, and B. Roturier, "Automatic gain control (AGC) as an interference assessment tool," in *Proc. Int. Tech. Meeting Satell. Division The Inst. Navigat. (ION GPS/GNSS)*, 2003, pp. 2042–2053.
[46] S. Thombre and J. Nurmi, "Bandpass-sampling based GNSS sampled data generator—A design perspective," in *Proc. Int. Conf. Localization GNSS (ICL-GNSS)*, 2012, pp. 1–6, doi: 10.1109/ICL-GNSS.2012.6253114.
[47] D. M. Akos, M. Stockmaster, J. B. Y. Tsui, and J. A. C. Caschera, "Direct bandpass sampling of multiple distinct RF signals," *IEEE Trans. Commun.*, vol. 47, no. 7, pp. 983–988, Jul. 1999, doi: 10.1109/26.774848.
[48] K. M. Pesyna, R. W. Heath, Jr., and T. E. Humphreys, "Precision limits of low-energy GNSS receivers," in *Proc. ION GNSS*, 2013, pp. 2828–2834.
[49] N. Linty, L. L. Presti, F. Dovis, and P. Crosta, "Performance analysis of duty-cycle power saving techniques in GNSS mass-market receivers," in *Proc. IEEE/ION Position, Location Navigat. Symp.*, May 2014, pp. 1096–1104, doi: 10.1109/PLANS.2014.6851479.
[50] T. Pany and B. Eissfeller, "Code and phase tracking of generic PRN signals with sub-nyquist sample rates," *Navigation*, vol. 51, no. 2, pp. 143–160, 2004.
[51] P. Axelrad, J. Donna, and M. Mitchell, "Enhancing GNSS acquisition by combining signals from multiple channels and satellites," in *Proc. ION GNSS*, 2009, pp. 2617–2628.
[52] C. Jiang, S. Chen, Y. Chen, and Y. Bo, "Research on a chip scale atomic clock aided vector tracking loop," *IET Radar Sonar Navig.*, vol. 13, no. 7, pp. 1101–1106, 2019.
[53] J.-H. Won, T. Pany, and B. Eissfeller, "Iterative maximum likelihood estimators for high-dynamic GNSS signal tracking," *IEEE Trans. Aerosp. Electron. Syst.*, vol. 48, no. 4, pp. 2875–2893, Oct. 2012.
[54] M. Lashley, D. M. Bevly, and J. Y. Hung, "Performance analysis of vector tracking algorithms for weak GPS signals in high dynamics," *IEEE J. Sel. Topics Signal Process.*, vol. 3, no. 4, pp. 661–673, Aug. 2009.
[55] Y. Ng and G. X. Gao, "GNSS multireceiver vector tracking," *IEEE Trans. Aerosp. Electron. Syst.*, vol. 53, no. 5, pp. 2583–2593, Oct. 2017.
[56] F. V. Diggelen, "Who's your daddy? Why GPS will continue to dominate consumer GNSS," in *Proc. InsideGNSS*, Apr. 2014, pp. 30–41.
[57] A. Molino, G. Girau, M. Nicola, M. Fantino, and M. Pini, "Evaluation of a FFT-based acquisition in real time hardware and software GNSS receivers," in *Proc. IEEE 10th Int. Symp. Spread Spectr. Techn. Appl.*, Aug. 2008, pp. 37–41.
[58] T. Kazukuni, F. Tetsuhiro, T. Katsuyuki, T. Katsumi, and M. Youssef, "Sonys CXD5603GF—The lowest power consumption GNSS chip in the IoT tracker market," in *Proc. 31st Int. Tech. Meeting Satell. Division Inst. Navigat.*, Oct. 2018, pp. 517–537.
[59] G. X. Gao, M. Sgammini, M. Lu, and N. Kubo, "Protecting GNSS receivers from jamming and interference," *Proc. IEEE*, vol. 104, no. 6, pp. 1327–1338, Jun. 2016.
[60] R. Morales-Ferre, P. Richter, E. Falletti, A. de la Fuente, and E. S. Lohan, "A survey on coping with intentional interference in satellite navigation for manned and unmanned aircraft," *IEEE Commun. Surveys Tuts.*, vol. 22, no. 1, pp. 249–291, 1st Quart., 2020.
[61] M. Z. H. Bhuiyan and E. S. Lohan, "Advanced multipath mitigation techniques for satellite-based positioning applications," *Int. J. Navigat. Observ.*, vol. 2010, pp. 1–15, Dec. 2010, doi: 10.1155/2010/412393.
[62] X. Chen, F. Dovis, S. Peng, and Y. Morton, "Comparative studies of GPS multipath mitigation methods performance," *IEEE Trans. Aerosp. Electron. Syst.*, vol. 49, no. 3, pp. 1555–1568, Jul. 2013.
[63] C. Günther, "A survey of spoofing and counter-measures," *Navigat. J. Inst. Navigat.*, vol. 61, no. 3, pp. 159–177, 2014.
[64] M. L. Psiaki and T. E. Humphreys, "GNSS spoofing and detection," *Proc. IEEE*, vol. 104, no. 6, pp. 1258–1270, Jun. 2016.
[65] D. Egea-Roca, G. Seco-Granados, J. A. Lopez-Salcedo, M. Moriana, E. Dominguez, E. Aguado, D. Lowe, D. Naberzhnykh, F. Dovis, I. Fernández-Hernández, and J. P. Boyero, "Signal-Level integrity and metrics based on the application of quickest detection theory to multipath detection," in *Proc. ION GNSS*, 2015, pp. 2926–2938.
[66] D. Egea-Roca, G. Seco-Granados, J. A. Lopez-Salcedo, E. Dominguez, E. Aguado, D. Lowe, D. Naberzhnykh, F. Dovis, I. Fernández-Hernández, and J. P. Boyero, "Signal-Level integrity and metrics based on the application of quickest detection theory to interference detection," in *Proc. ION GNSS*, 2015, pp. 3136–3147.
[67] D. Egea-Roca, J. A. Lopez-Salcedo, G. Seco-Granados, and H. V. Poor, "Performance bounds for finite moving average tests in transient change detection," *IEEE Trans. Signal Process.*, vol. 66, no. 6, pp. 1594–1606, Mar. 2018.
[68] I. Fernandez, V. Rijmen, T. Ashur, P. Walker, G. Seco, J. Simon, C. Sarto, D. Burkey, and O. Pozzobon, "GALILEO navigation message authentication specification for signal-in-space testing–V1. 0," Eur. Commission, Brussels and Luxembourg, Tech. Rep. 1, Nov. 2016.
[69] *Chip Message Robust Authentication (Chimera) Enhancement for the L1C Signal: Space Segment/User Segment Interface*, document IS-AGT-100, Apr. 2019.
[70] L. Scott, "Anti-spoofing & authenticated signal architectures for civil navigation systems," in *Proc. ION GPS/GNSS*, 2003, pp. 1543–1552.
[71] D. Margaria, B. Motella, M. Anghileri, J.-J. Floch, I. Fernandez-Hernandez, and M. Paonni, "Signal structure-based authentication for civil GNSSs: Recent solutions and perspectives," *IEEE Signal Process. Mag.*, vol. 34, no. 5, pp. 27–37, Sep. 2017.
[72] D. Borio, C. Gioia, E. Cano-Pons, and G. Baldini, "Feature selection for GNSS receiver fingerprinting," in *Proc. InsideGNSS*, Jul./Aug. 2017, pp. 54–61.
[73] A. Jafarnia-Jahromi, A. Broumandan, J. Nielsen, and G. Lachapelle, "GPS vulnerability to spoofing threats and a review of antispoofing techniques," *Int. J. Navigat. Observ.*, vol. 2012, pp. 1–16, Jul. 2012, doi: 10.1155/2012/127072.
[74] N. Zhu, J. Marais, D. Betaille, and M. Berbineau, "GNSS position integrity in urban environments: A review of literature," *IEEE Trans. Intell. Transp. Syst.*, vol. 19, no. 9, pp. 2762–2778, Sep. 2018.
[75] D. Egea-Roca, "Change detection techniques for GNSS signal-level integrity," Ph.D. dissertation, Dpt. Telecommu. Syst. Eng., Univ. Autònoma de Barcelona, Cincinnati, OH, USA, 2017.
[76] E. Shytermeja and A. Garcia-Pena, "Proposed architecture for integrity monitoring of a GNSS/MEMS system with a fisheye camera in urban environment," in *Proc. ICL-GNSS*, Jun. 2014, pp. 1–6, doi: 10.1109/ICL-GNSS.2014.6934179.
[77] R. Toledo-Moreo, B. Úbeda, J. Santa, M. A. Zamora-Izquierdo, and A. F. Gómez-Skarmeta, "An analysis of positioning and map-matching issues for GNSS-based road user charging," in *Proc. 13th Int. Conf. Intell. Trans. Syst.*, 2010, pp. 1486–1491.
[78] U. I. Bhatti and W. Y. Ochieng, "Detecting multiple failures in GPS/INS integrated system: A novel architecture for integrity monitoring," *J. Global Positioning Syst.*, vol. 8, no. 1, pp. 26–42, Jun. 2009.
[79] J. A. del Peral-Rosado, J. Saloranta, G. Destino, J. A. López-Salcedo, and G. Seco-Granados, "Methodology for simulating 5G and GNSS high-accuracy positioning," *Sensors*, vol. 18, Art. no. 10, pp. 3220–3244, Sep. 2018.
[80] G. J. Geier, T. M. King, H. L. Kennedy, R. D. Thomas, and B. R. McNamara, "Prediction of the time accuracy and integrity of GPS timing," in *Proc. IEEE Int. Freq. Control Symp.*, Dec. 1995, pp. 266–274.
[81] P. Vyskocil and J. Sebesta, "Relative timing characteristics of GPS timing modules for time synchronization application," in *Proc. IEEE Int. Workshop Satell. Space Commun.*, Aug. 2009, pp. 230–234.
[82] C. Gioia and B. Daniele, "Multi-Constellation T-RAIM: An experimental evaluation," in *Proc. ION GNSS*, Portland, Oregon, Sep. 2017, pp. 4248–4256.
[83] G. Fu, T. Holmes, C. Riedel, and J. Liu, "RAIM and SBAS based detection of GNSS spoofing by timing and content consistency rules," in *Proc. ION GNSS*, 2017, pp. 2854–2868.
[84] I. Fernández-Hernández, T. Senni, D. Borio, and G. Vecchione, "High-parity vertical Reed–Solomon codes for long GNSS high-accuracy messages," *Navigat.*, vol. 67, no. 2, pp. 365–378, 2020.

[85] E. Wang, T. Yang, Z. Wang, Y. Zhang, J. Guo, W. Shu, and P. Qu, "Performance evaluation of precise point positioning for beiDou-3 B1c/B2a signals in the global range," *Sensors*, vol. 21, no. 17, pp. 5780–5796, Aug. 2021.

[86] J. S. Booth and R. N. Snow, "An evaluation of omnistar XP and PPP as a replacement fo DGPS in airborne applications," in *Proc. ION GNSS*, Savannah, GA, USA, Sep. 2009, pp. 1188–1194.

[87] C. Rodriguez-Solano, N. Talbot, G. Zyryanov, X. Chen, K. Doucet, L. Goercke, S. Junker, H. Landau, N. Reussner, and D. Sampaio, "Protection level of the trimble RTX positioning engine for autonomous applications," in *Proc. ION GNSS*, St. Louis, MI, USA, Sep. 2021, pp. 1577–1595.

[88] M. Jones, *Anti-Jam technology: Demystifying the CRPA*. Chennai, India: GPS World, 2017. Accessed: Nov. 24, 2021. [Online]. Available: https://www.gpsworld.com/anti-jam-technology-demystifying-the-crpa/

[89] F. Troetschel, F. Antreich, and J. A. Nossek, "Space-time adaptive principle component analysis for time-delay estimation," in *Proc. Sensor Array Multichannel Signal Process. Workshop (SAM)*, 2014, pp. 105–108.

[90] M. Da Rosa Zanatta, J. P. C. L. Da Costa, F. Antreich, M. Haardt, G. Elger, F. L. Lopes De Mendonca, and R. T. De Sousa, "Tensor-based framework with model order selection and high accuracy factor decomposition for time-delay estimation in dynamic multipath scenarios," *IEEE Access*, vol. 8, pp. 174931–174942, 2020, doi: 10.1109/ACCESS.2020.3024597.

[91] G. Seco-Granados, J. A. Fernandez-Rubio, and C. Fernandez-Prades, "ML estimator and hybrid beamformer for multipath and interference mitigation in GNSS receivers," *IEEE Trans. Signal Process.*, vol. 53, no. 3, pp. 1194–1208, Mar. 2005.

[92] M. Appel, A. Iliopoulos, F. Fohlmeister, E. Pérez Marcos, M. Cuntz, A. Konovaltsev, F. Antreich, and M. Meurer, "Interference and multipath suppression with space-time adaptive beamforming for safety-of-life maritime applications," *CEAS Space J.*, vol. 11, no. 1, pp. 21–34, Mar. 2019.

[93] M. da Rosa Zanatta, F. L. Lópes de Mendonça, F. Antreich, D. Valle de Lima, R. Kehrle Miranda, G. Del Galdo, and J. P. C. L. da Costa, "Tensor-based time-delay estimation for second and third generation global positioning system," *Digit. Signal Process.*, vol. 92, pp. 1–19, Sep. 2019, doi: 10.1016/j.dsp.2019.04.003.

[94] J. Selva, "An efficient Newton-type method for the computation of ML estimators in a uniform linear array," *IEEE Trans. Signal Process.*, vol. 53, no. 6, pp. 2036–2045, Jun. 2005.

[95] F. Antreich, J. A. Nossek, G. Seco-Granados, and A. L. Swindlehurst, "The extended invariance principle for signal parameter estimation in an unknown spatial field," *IEEE Trans. Signal Process.*, vol. 59, no. 7, pp. 3213–3225, Jul. 2011, doi: 10.1109/TSP.2011.2140107.

[96] F. Antreich, J. A. Nossek, and W. Utschick, "Maximum likelihood delay estimation in a navigation receiver for aeronautical applications," *Aerosp. Sci. Technol.*, vol. 12, no. 3, pp. 256–267, Apr. 2008, doi: 10.1016/j.ast.2007.06.005.

[97] M. Jones. *Anti-Jam Systems: Which One Works for You*. Chennai, India: GPS World, 2017. Accessed: Nov. 24, 2021. [Online]. Available: https://www.gpsworld.com/anti-jam-systems-which-one-works-for-you/

[98] *GPSdome*. Accessed: Nov. 24, 2021. [Online]. Available: https://www.infinidome.com/?lang=es

[99] E. Perez-Marcos, L. Kurz, M. Cuntz, S. Caizzone, A. Konovaltsev, and M. Meurer, "ITAR free smart antenna array for resilient GNSS in Aviation," in *Proc. IEEE/ION PLANS*, Feb. 2020, pp. 606–611.

[100] M. Appel, A. Iliopoulos, F. Fohlmeister, E. Pérez Marcos, M. Cuntz, A. Konovaltsev, F. Antreich, and M. Meurer, "Experimental validation of GNSS repeater detection based on antenna arrays for maritime applications," *CEAS Space J.*, vol. 11, no. 1, pp. 7–19, Mar. 2019.

[101] A. Konovaltsev, L. A. Greda, M. Heckler, and A. Hornbostel, "Phase center variations in adaptive GNSS antenna arrays," presented at the NAVITEC, 2008. Accessed: Feb. 12, 2022. [Online]. Available: https://pdfs.semanticscholar.org/a493/1a595d875c5bf4737f 6ffa3ed8b 3597597c3db7.pdf

[102] M. Sgammini, F. Antreich, L. Kurz, M. Meurer, and T. G. Noll, "Blind adaptive beamformer based on orthogonal projections for GNSS," in *Proc. ION GNSS*, 2012, pp. 926–935.

[103] B. Hammoud, F. Antreich, J. A. Nossek, J. P. C. L. D. Costa, and A. L. F. D. Almeida, "Tensor-based approach for time-delay estimation," in *Proc. Int. ITG Workshop Smart Antennas (WSA)*, 2016, pp. 1–7.

[104] M. Sgammini, F. Antreich, and M. Meurer, "SVD-based RF interference detection and mitigation for GNSS," in *Proc. ION GNSS*, 2014, pp. 3475–3483.

[105] A. Iliopoulos, C. Enneking, O. G. Crespillo, T. Jost, M. Appel, and F. Antreich, "Robust GNSS ranging in the presence of repeater signals," in *Proc. ION GNSS*, 2017, pp. 3941–3957.

[106] N. Blanco-Delgado and F. D. Nunes, "Multipath estimation in multicorrelator GNSS receivers using the maximum likelihood principle," *IEEE Trans. Aerosp. Electron. Syst.*, vol. 48, no. 4, pp. 3222–3233, Oct. 2012.

[107] P. Closas, C. Fernandes-Prades, and J. A. Fernandes-Rubio, "A particle filtering tracking algorithm for GNSS synchronization using Laplace's method," in *Proc. IEEE Int. Conf. Acoust., Speech Signal Process. (ICASSP)*, Dec. 2008, pp. 3409–3412.

[108] B. Krach, M. Lentmaier, and P. Robertson, "Joint Bayesian positioning and multipath mitigation in GNSS," in *Proc. ICASSP*, 2008, pp. 3437–3440.

[109] C. Enneking and F. Antreich, "Exploiting WSSUS multipath for GNSS Ranging," *IEEE Trans. Veh. Technol.*, vol. 66, no. 9, pp. 7663–7676, Sep. 2017.

[110] A. Konovaltsev, M. Cuntz, C. Haettich, and M. Meurer, "Autonomous spoofing detection and mitigation in a GNSS receiver with an adaptive antenna array," in *Proc. ION GNSS*, 2013, pp. 2937–2948.

[111] D. S. De Lorenzo, F. Antreich, H. Denks, A. Hornbostel, C. Weber, and P. Enge, "Testing of adaptive beamsteering for interference rejection in GNSS receivers," in *Proc. ENC*, 2007, pp. 1–5. Accessed: Feb. 12, 2022. [Online]. Available: https://citeseerx.ist.psu.edu/viewdoc/download?doi=10.1.1.298.9957&rep=rep1&type=pdf

[112] L. Kurz, E. Tasdemir, D. Bornkessel, T. G. Noll, G. Kappen, F. Antreich, M. Sgammini, and M. Meurer, "An architecture for an embedded antenna-array digital GNSS receiver using subspace-based methods for spatial filtering," in *Proc. NAVITEC*, 2012, pp. 1–8, doi: 10.1109/NAVITEC.2012.6423050.

[113] M. H. Castaneda, M. Stein, F. Antreich, E. Tasdemir, L. Kurz, T. G. Noll, and J. A. Nossek, "Joint space-time interference mitigation for embedded multi-antenna GNSS receivers," in *Proc. ION GNSS*, 2013, pp. 3399–3408.

[114] E. Tasdemir, L. Kurz, and T. G. Noll, "Optimization of a blind adaptive spatial filter for interference mitigation in GNSS receivers," in *Proc. ION GNSS*, 2013, pp. 3424–3432.

[115] A. Konovaltsev, D. De Lorenzo, A. Hornbostel, and P. Enge, "Mitigation of continuous and pulsed radio interference with GNSS antenna arrays," in *Proc. ION GNSS*, 2008, pp. 2786–2795.

[116] M. Sgammini, S. Caizzone, A. Hornbostel, and M. Meurer, "Interference mitigation using a dual-polarized antenna array in a real environment," *Navigation*, vol. 66, no. 3, pp. 523–535, 2019.

[117] L. Scott, "GNSS solutions: Signal acquisition and search and antenna polarization," in *Proc. InsideGNSS*, Mar./Apr. 2007, pp. 26–33.

[118] D. Aloi and F. Van Graas, "Ground-multi path mitigation via polarization steering of GPS signal," *IEEE Trans. Aerosp. Electron. Syst.*, vol. 40, no. 2, pp. 536–552, Jul. 2004.

[119] P. D. Groves, Z. Jiang, B. Skelton, and P. A. Cross, "Novel multipath mitigation methods using a dual-polarization antenna," in *Proc. ION GNSS*, 2010, pp. 140–151.

[120] F. Fohlmeister, A. Iliopoulos, M. Sgammini, F. Antreich, and J. A. Nossek, "Dual polarization beamforming algorithm for multipath mitigation in GNSS," *Signal Process.*, vol. 138, pp. 86–97, Sep. 2017, doi: 10.1016/j.sigpro.2017.03.012.

[121] F. Wendler, F. Antreich, J. A. Nossek, and A. L. Swindlehurst, "Dual-polarization time delay estimation for multipath mitigation," in *Proc. WSA*, 2015, pp. 1–6.

[122] F. Wendler, F. Antreich, J. A. Nossek, and A. L. Swindlehurst, "Stochastic-deterministic multipath model for time-delay estimation," in *Proc. WSA*, 2016, pp. 1–6.

[123] D. V. Lima, J. P. C. L. da Costa, F. Antreich, R. K. Miranda, and G. del Galdo, "High resolution time-delay estimation via direction of arrival estimation and Khatri-Rao factorization for multipath mitigation," in *Proc. WSA*, 2017, pp. 1–8.

[124] D. V. Lima, J. P. C. L. da Costa, F. Antreich, and G. del Galdo, "Time-delay estimation via CPD-GEVD applied to tensor-based GNSS arrays with errors," in *Proc. IEEE Int. Workshop Comput. Adv. Multi-Sensor Adapt. Process. (CAMSAP)*, Dec. 2017, pp. 1–5, doi: 10.1109/CAMSAP.2017.8313098.

[125] R. Anderson, H. R. Bilger, and G. E. Stedman, ''Sagnac effect: A century of Earth-rotated interferometers,'' *Amer. J. Phys.*, vol. 62, no. 11, pp. 975–985, 1994.
[126] N. M. Barbour, R. Hopkins, A. Kourepenis, and P. Ward, ''Inertial MEMS system applications,'' NATO, Washington, DC, USA, Tech. Rep. RTO-EN-SET-116, 2011.
[127] J. Farrell and B. Matthew, *The Global Positioning System and Inertial Navigation*. New York, NY, USA: McGraw-Hill, 1999.
[128] D. Feng, ''Review of quantum navigation,'' *IOP Conf. Ser., Earth Environ. Sci.*, vol. 237, no. 3, pp. 1–10, 2019, doi: 10.1088/1755-1315/237/3/032027.
[129] B. J. Little, G. W. Hoth, J. Christensen, C. Walker, D. J. De Smet, G. W. Biedermann, J. Lee, and P. D. D. Schwindt, ''A passively pumped vacuum package sustaining cold atoms for more than 200 days,'' *AVS Quantum Sci.*, vol. 3, no. 3, pp. 1–6, 2021, doi: 10.1116/5.0053885.
[130] S. Sand, A. Dammann, and C. Mensing, *Positioning Wireless Communication Systwm*. Hoboken, NJ, USA: Wiley, May 2014.
[131] F. Forno, G. Malnati, and G. Portelli, ''Design and implementation of a Bluetooth ad-hoc network for indoor positioning,'' *IEEE Proc.-Softw.*, vol. 125, no. 5, pp. 223–228, Dec. 2005.
[132] A. Mahtab Hossain, Y. Jin, W. S. Soh, and H. N. Van, ''SSD: A robust RF location fingerprint addressing mobile devices' heterogeneity,'' *IEEE Trans. Mobile Comp.*, vol. 12, no. 1, pp. 65–77, Oct. 2013.
[133] InSoft GmbH. *Bluetooth Low-Energy Beacons*. Accessed: Nov. 24, 2021. [Online]. Available: https://www.infsoft.com/technology/sensors/bluetooth-low-energy-beacons
[134] POLE STAR. *The Best-in-Class Indoor Location Technology*. Accessed: Nov. 24, 2021. [Online]. Available: https://www.polestar.eu/
[135] Teldio. *Real-Time Location System*. Accessed: Nov. 24, 2021. [Online]. Available: https://www.teldio.com/products/rtls/
[136] J. Tiemann, F. Schweikowski, and C. Wietfeld, ''Design of an UWB indoor-positioning system for UAV navigation in GNSS-denied environments,'' in *Proc. Int. Conf. Indoor Positioning Indoor Navigat. (IPIN)*, 2015, pp. 1–8, doi: 10.1109/IPIN.2015.7346960.
[137] C. Rizos and Y. Ling, ''Background and recent advances in the Locata terrestrial positioning and timing technology,'' *Sensors*, vol. 19, no. 8, pp. 1821–1840, 2019, doi: 10.3390/s19081821.
[138] A. Ren, F. Zhou, A. Rahman, X. Wang, N. Zhao, and X. Yang, ''A study of indoor positioning based on UWB base-station configurations,'' in *Proc. IEEE 2nd Adv. Inf. Technol., Electron. Autom. Control Conf. (IAEAC)*, Mar. 2017, pp. 1939–1943.
[139] C. Rizos, G. Roberts, J. Barnes, and N. Gambale, ''Experimental results of Locata: A high accuracy indoor positioning system,'' in *Proc. IPIN*, Sep. 2010, pp. 1–7, doi: 10.1109/IPIN.2010.5647717.
[140] A. P. Iannucci and E. T. Humphreys, ''Economical fused LEO GNSS,'' in *Proc. PLANS*, 2020, pp. 426–443.
[141] Z. Kassas, J. Morales, and J. Khalife, ''New-age satellite-based navigation–STAN: Simultaneous tracking and navigation with LEO satellite signals,'' in *Proc. InsideGNSS*, 2019, pp. 56–65.
[142] T. G. Reid, A. M. Neish, T. Walter, and P. K. Enge, ''Broadband LEO constellations for navigation,'' *Navigation*, vol. 65, no. 2, pp. 205–220, 2018.
[143] J. A. del Peral-Rosado, R. Raulefs, J. A. López-Salcedo, and G. Seco-Granados, ''Survey of cellular mobile radio localization methods: From 1G to 5G,'' *IEEE Commun. Surveys Tuts.*, vol. 20, no. 2, pp. 1124–1148, 2nd Quart., 2017.
[144] C. Botteron, E. Firouzi, and P. A. Farine, ''Performance analysis of mobile station location using hybrid GNSS and cellular network measurements,'' in *Proc. ION GNSS*, 2004, pp. 2458–2467.
[145] *Physical channels and modulation*, document TS 36.211 9, 3GPP, 2010.
[146] H. Wymeersch, G. Seco-Granados, G. Destino, D. Dardari, and F. Tufvesson, ''5G mm-Wave positioning for vehicular networks,'' *IEEE Wireless Commun. Mag.*, vol. 24, no. 6, pp. 80–86, Oct. 2017.
[147] *Study on Positioning Use Cases*, document TR22.872 16, 3GPP, Jun. 2018.
[148] J. A. del Peral-Rosado, R. Estatuet, J. A. López-Salcedo, G. Seco-Granados, Z. Chaloupka, L. Ries, and J. A. Garcia Molina, ''Evaluation of hybrid positioning scenarios for autonomous vehicle applications,'' in *Proc. ION GNSS*, 2017, pp. 2541–2553.
[149] A. Zaidi, R. Baldemair, and H. Tullberg, ''Waveform and numerology to support 5G services and requirements,'' *IEEE Commun. Mag.*, vol. 5, no. 11, pp. 90–98, Dec. 2016.
[150] Z. E. Ankarali, B. Peköz, and H. Arslan, ''Flexible radio access beyond 5G: A future projection on waveform, numerology, and frame design principles,'' *IEEE Access*, vol. 5, pp. 18295–18309, 2017, doi: 10.1109/ACCESS.2017.2684783.
[151] M. Mueck, E. Strinati, and I. Kim, ''5G CHAMPION–rolling out 5G in 2018,'' in *Proc. IEEE Globecom Workshops (GC Wkshps)*, Dec. 2016, pp. 1–6, doi: 10.1109/GLOCOMW.2016.7848798.
[152] *New SID: Study on NR Positioning Support*, document TSG RAN Meeting #80, RP-180897, 3GPP, 2018.
[153] A. A. Adebomehin and S. D. Walker, ''Enhanced ultrawideband methods for 5G LOS sufficient positioning and mitigation,'' in *Proc. IEEE 17th Int. Symp. A World Wireless, Mobile Multimedia Netw. (WoWMoM)*, Jun. 2016, pp. 1–4, doi: 10.1109/WoWMoM.2016.7523540.
[154] G. Wang, H. Chen, Y. Li, and N. Ansari, ''NLOS error mitigation for TOA-based localization via convex relaxation,'' *IEEE Trans. Wireless Commun.*, vol. 13, no. 8, pp. 4119–4131, Aug. 2014.
[155] G. Hein, J. Avila-Rodriguez, and S. Wallner, ''MBOC: The new optimized spreading modulation recommended for GALILEO L1 OS and GPS L1C,'' in *Proc. PLANS*, 2006, pp. 883–892.
[156] T. Yan, J. Wei, Z. Tang, Z. Zhou, and X. Xia, ''General AltBOC modulation with adjustable power allocation ratio for GNSS,'' *J. Navigat.*, vol. 69, no. 3, pp. 531–560, May 2016.
[157] J. T. Curran, M. Navarro, M. Anghileri, P. Closas, and S. Pfletschinger, ''Coding aspects of secure GNSS receivers,'' *Proc. IEEE*, vol. 104, no. 6, pp. 1271–1287, Jun. 2016.
[158] M. Jones, ''The civilian battlefield. Protecting GNSS receivers from interference jamming,'' in *Proc. InsideGNSS*, Mar./Apr. 2011, pp. 40–49.
[159] S.-H. Kong, ''High sensitivity and fast acquisition signal processing techniques for GNSS receivers: From fundamentals to state-of-the-art GNSS acquisition technologies,'' *IEEE Signal Process Mag.*, vol. 34, no. 5, pp. 59–71, Sep. 2017.
[160] Z. Zhuang, K.-H. Kim, and J. P. Singh, ''Improving energy efficiency of location sensing on smartphones,'' in *Proc. Int. Conf. Mobile Syst., Appl., Services*, 2010, pp. 315–330, doi: 10.1145/1814433.1814464.
[161] G. W. Hein, T. Pany, S. Wallner, and J. H. Woon, ''Platforms for a future GNSS receiver: A discussion of ASIC, FPGA, and DSP technologies,'' in *Proc. InsideGNSS*, Mar./Apr. 2006, pp. 56–62.
[162] M. G. Petovello, C. O'Driscoll, G. Lachapelle, D. Borio, and H. Murtaza, ''Architecture and benefits of an advanced GNSS software receiver,'' in *Proc. Int. Symp. GPS/GNSS*, 2008, pp. 156–168.
[163] T. Pany, D. Dötterböck, H. Gomez-Martinez, M. S. Hammed, F. Hörkner, T. Kraus, D. Maier, D. Sanchez-Morales, A. Schütz, P. Klima, and D. Ebert, ''The multi-sensor navigation analysis tool (MuSNAT)-architecture, LiDAR, GPU/CPU GNSS signal processing,'' in *Proc. ION GNSS*, 2019, pp. 4087–4115.
[164] J. Dampf, T. Pany, W. Bär, J. Winkel, C. Stöber, K. Fürlinger, P. Closas, and J. A. Garcìa-Molina, ''More than we ever dreamed possible: Processor technology for GNSS software receivers in the year 2015,'' in *InsideGNSS*, Jul./Aug. 2015, pp. 62–72.
[165] P. Galambos, ''Cloud, fog, and mist computing: Advanced robot applications,'' *IEEE Syst., Man, Cybern. Mag.*, vol. 6, no. 1, pp. 41–45, Jan. 2020.
[166] S. S. Gill and R. Buyya, ''Failure management for reliable cloud computing: A taxonomy, model, and future directions,'' *Comput., Sci. Eng. Mag.*, vol. 22, no. 3, pp. 52–63, 2020.
[167] J. Zhang, Z. Chen, Z. Xu, M. Du, W. Yang, and L. Guo, ''A distributed collaborative urban traffic big data system based on cloud computing,'' *IEEE Intell. Transp. Syst. Mag.*, vol. 11, no. 4, pp. 37–47, Oct. 2019.
[168] V. Lucas-Sabola, G. Seco-Granados, J. A. López-Salcedo, J. A. García-Molina, and M. Crirsci, ''Efficiency analysis of cloud GNSS signal processing IoT applications,'' in *Proc. ION GNSS*, 2017, pp. 3843–3852.
[169] V. Lucas-Sabola, G. Seco-Granados, J. A. López-Salcedo, J. A. García-Molina, and M. Crirsci, ''Demonstration of cloud GNSS signal processing,'' in *Proc. ION GNSS*, 2016, pp. 34–43.
[170] Rokubun. *JASON PaaS*. Accessed: Nov. 24, 2021. [Online]. Available: https://www.rokubun.cat/gnss-cloud/
[171] S. N. Sadrieh and M. H. Afzal, ''XYBRID CLOUD: A cloud based GNSS receiver,'' in *Proc. IPIN*, 2015, pp. 1–8, doi: 10.1109/IPIN36528.2015.
[172] Swift Navigation. *Skylark Cloud Correction Service*. Accessed: Nov. 24, 2021. [Online]. Available: https://www.swiftnav.com/skylark
[173] K. V. Dierendonck, O. Al-Fanek, and M. Petovello, ''What is snapshot positioning and what advantages does it offer?'' in *Proc. InsideGNSS*, Nov./Dec. 2018, pp. 28–32.

[174] V. Lucas-Sabola, G. Seco-Granados, J. A. López-Salcedo, and J. A. García-Molina, "Performance analysis of low-power GNSS positioning in IoT," in *Proc. NAVITEC*, 2018, pp. 1–4, doi: 10.1109/NAVITEC45235.2018.
[175] Baseband Technologies. *Snapshot Receiver*. Accessed: Nov. 24, 2021. [Online]. Available: https://www.basebandtech.com/ultra-low-power-receiver/
[176] D. Dötterböck and B. Eissfeller, "A GPS/Galileo software snapshot receiver for mobile phones," in *Proc. Int. Assoc. Inst. Navigat. (IAIN)*, 2009, pp. 1–5. Accessed: Feb. 12, 2022. [Online]. Available: https://www.semanticscholar.org/paper/A-GPS%2FGalileo-Software-Snap-Shot-Receiver-for-Dötterböck-Eissfeller/4440fee7d995b5bb1ba00ed07e9e00431d3068c5
[177] *Using GNSS Raw Measurements on Android Devices*, GSA, Prague, Czech republic, 2017.
[178] D. Gómez-Casco, J. A. López-Salcedo, and G. Seco-Granados, "Generalized integration techniques for high-sensitivity GNSS receivers affected by oscillator phase noise," in *Proc. IEEE Stat. Signal Process. Workshop (SSP)*, Jun. 2016, pp. 1–5, doi: 10.1109/SSP.2016.7551809.
[179] M. Zhang and J. Zhang, "A fast satellite selection algorithm: Beyond four satellites," *IEEE J. Sel. Topics Signal Process.*, vol. 3, no. 2, pp. 740–747, Oct. 2009.
[180] T. Soinien, P. Syrjärinne, S. Ali-Löytty, and C. Schmid, "Data-driven approach to satellite selection in multi-constellation GNSS receivers," in *Proc. ICL-GNSS*, 2018, pp. 1–6, doi: 10.1109/ICL-GNSS.2018.8440912.
[181] Y. Henri and A. Matas, "RNSS and the ITU radio regulations," in *Proc. InsideGNSS*, Jan./Feb. 2018, pp. 32–39.
[182] *Portables: The Challenge of Low Power and Good GNSS Performance*, U-Blox, Thaiwii, Switzerland, 2017.
[183] C. Abraham, S. de la Porte, and S. Podshivalov, "Method and apparatus for performing signal correlation," U.S. Patent 7 190 712 B2, Mar. 13, 2007.
[184] C. Abraham, "Method and apparatus for performing signal correlation using historical correlation data," U.S Patent 6 819 707 B2, Jul. 15, 2009.
[185] L. Young and A. Reza, *SiRF Application Note Power Management Considerations of Sirfs-TarIII*. San José, CA, USA: SiRF Technol., 2005.
[186] *JF2/JN3 Low Power Modes*, Telit Communications, London, U.K., 2012.
[187] Broadcom Products. *BCM47765 Second Generation Dual-Frequency GNSS Chip*. Accessed: Nov. 24, 2021. [Online]. Available: https://www.broadcom.com/products/wireless/gnss-gps-socs/bcm47765
[188] U-Blox. *Product Summary MAX-M10 Series U-Blox M10 Standard Precision GNSS Modules*. Accessed: Nov. 24, 2021. [Online]. Available: https://www.u-blox.com/en/product/max-m10-series#tab-documentation-resources
[189] U-Blox. *Product Summary ZED-F9R Module U-Blox F9 High Precision Dead Reckoning Module*. Accessed: Nov. 24, 2021. [Online]. Available: https://www.u-blox.com/en/product/zed-f9r-module#tab-documentation-resources
[190] STMicroelectronics. *STA8100GA TeseoV Multi Frequency GNSS Receiver*. Accessed: Nov. 24, 2021. [Online]. Available: https://www.st.com/en/automotive-infotainment-and-telematics/sta8100ga.html

DANIEL EGEA-ROCA (Member, IEEE) received the M.Sc. and Ph.D. degrees in electrical engineering from Universitat Autònoma de Barcelona (UAB), Bellaterra, Barcelona, Spain, in 2012 and 2017, respectively. During his Ph.D. studies, he was involved in research projects funded by the European Commission (EC) and GSA. Furthermore, he received several appointments, such as Princeton University (USA), hosted by Prof. H. Vincent Poor, and Hanyang University (South Korea), hosted by Prof. Sunwoo Kim. In 2017, he joined the Department of Telecommunications and Systems Engineering, UAB, as a Postdoctoral Researcher. Since 2017, he has been involved in several research projects funded by the EC and the European Space Agency (ESA) awards. He has authored approximately 20 publications and received three best papers/presentations. His research interests include the area of signal processing and its application in threat detection and integrity techniques for GNSS receivers. In recent years, he has been involved in GNSS signal design research.

MARKEL ARIZABALETA-DIEZ received the M.Sc. degree in electrical engineering from Euskal Herriko Unibertsitatea (UPV-EHU), Bilbao, Spain, in 2017. He joined the Tampere University of Technology (TAU), Tampere, Finland, where he was involved in joint 5G communication and positioning systems. In July 2017, he joined the Navigation Unit LRT 9.2, Institute of Space Technology and Space Applications (ISTA), Universität der Bundeswehr München (UniBw M) as a Research Associate, and since 2017, he has been involved in projects for the European Commission and the European Space Agency (ESA). His research interests include the area of GNSS signal processing, including GNSS spoofing detection and signal authentication and 4G/5G positioning.

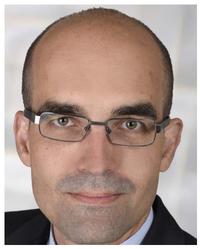

THOMAS PANY (Member, IEEE) received the Ph.D. degree from the Graz University of Technology (sub auspiciis). He worked in the GNSS industry for seven years. He is with the Space Systems Research Center (FZ-Space), Universität der Bundeswehr München, where he leads the Satellite Navigation Unit LRT 9.2 of the Institute of Space Technology and Space Applications (ISTA). He teaches navigation focusing on GNSS, sensor fusion and aerospace applications. Within LRT 9.2, a dozen full-time researchers investigate GNSS systems and signal design, GNSS transceivers and high-integrity multisensor navigation (inertial, LiDAR) and are also developing a modular UAV-based GNSS test bed. ISTA has also developed the MuSNAT GNSS software receiver and recently focused on smartphone positioning and GNSS/5G integration. He has authored approximately 200 publications, including one monography, and received five best presentation awards from the U.S. Institute of Navigation. He also organized the Munich Satellite Navigation Summit.

FELIX ANTREICH (Senior Member, IEEE) received the Diploma degree in electrical engineering and the Ph.D. degree from the Technical University of Munich (TUM), Munich, Germany, in 2003 and 2011, respectively. From 2003 to 2016, he was an Associate Researcher at the Department of Navigation, Institute of Communications and Navigation of the German Aerospace Center (DLR), Wessling, Germany. From 2016 to 2018, he was a Visiting Professor at the Department of Teleinformatics Engineering (DETI), Federal University of Ceará (UFC), Fortaleza, Brazil. Since July 2018, he has been a Professor with the Department of Telecommunications, Division of Electronics Engineering, Aeronautics Institute of Technology (ITA), São José dos Campos, Brazil. His research interests include sensor array signal processing for global navigation satellite systems (GNSS) and wireless communications, estimation theory, wireless sensor networks, positioning, localization, and signal design for synchronization.

JOSÉ A. LÓPEZ-SALCEDO (Senior Member, IEEE) received the Ph.D. degree in telecommunication engineering from Universitat Politècnica de Catalunya (UPC), in 2007. In 2006, he joined the Department of Telecommunication and Systems Engineering, Universitat Autònoma de Barcelona (UAB), where he is currently a Professor and served as Coordinator of the Telecommunications Engineering degree, from 2011 to 2019. He is the Principal Investigator of more than 15 research projects, most of them funded by the European Space Agency (ESA) on topics dealing with signal processing for GNSS receivers. He has held several visiting appointments at the Coordinated Science Laboratory, University of Illinois Urbana–Champaign, the University of California at Irvine, Hanyang University, and the European Commission Joint Research Center. He is also with the Institute of Spatial Studies of Catalonia (IEEC). His research interests include signal processing for communications and navigation, with special emphasis on cloud GNSS signal processing and the convergence between GNSS and 5G terrestrial cellular networks. He is the Secretary and Treasurer of the Spain Chapter of the IEEE Aerospace and Electronic Systems Society and a member of the Editorial Committee of the Korean Institute of Positioning, Navigation and Timing (IPNT).

MATTEO PAONNI received the B.S. degree in information engineering and the M.S. degree in electrical engineering from the University of Perugia, Italy. From 2007 to 2013, he was a Research Associate at the Institute of Space Technology and Space Applications, Universität der Bundeswehr München, Germany. He is currently a Project Manager with the Directorate for Space, Security and Migration, Joint Research Centre, European Commission, Ispra, Italy. Under his position, he provides technical and policy support to the EU Satellite Navigation Programmes Directorate within the European Commission and to the European GNSS Agency. His research interests include GNSS signal design and optimization, GNSS security, compatibility, and signal processing.

GONZALO SECO-GRANADOS (Senior Member, IEEE) received the Ph.D. degree in telecommunications engineering from the Universitat Politècnica de Catalunya, Spain, in 2000, and the M.B.A. degree from the IESE Business School, Spain, in 2002. He is currently a Professor with the Department of Telecommunication, Universitat Autònoma de Barcelona, where he served as Coordinator of the Telecommunications Engineering degree, from 2007 to 2010 and as the Vice Dean of the Engineering School, from 2011 to 2019. In 2015 and 2019, he was a Fulbright Visiting Scholar at the University of California, Irvine, USA. He is also with the Institute of Spatial Studies of Catalonia (IEEC). He has more than 300 publications in his research areas and holds three related patents. His research interests include GNSS, 5G, and beyond 5G localization. From 2002 to 2005, he was a member of the European Space Agency, where he was involved in the design of the Galileo System, and he. Since 2018, he has been serving as a member of the Sensor Array and Multichannel Technical Committee for the IEEE Signal Processing Society. Since 2019, he has been President of the Spanish Chapter of the IEEE Aerospace and Electronic Systems Society.